

# Statistical modelling of summary values leads to accurate Approximate Bayesian Computations

Oliver Ratmann

*Department of Infectious Disease Epidemiology, Imperial College London, Norfolk Place, London W2 1PG, UK. [oliver.ratmann@imperial.ac.uk](mailto:oliver.ratmann@imperial.ac.uk)*

Anton Camacho

*London School of Hygiene and Tropical Medicine, Keppel Street, London WC1E 7HT, UK*

Adam Meijer

*RIVM, National Institute for Public Health and the Environment, Centre for Infectious Disease Control, Bilthoven, The Netherlands*

Gé Donker

*NIVEL, Netherlands Institute for Health Services Research, P.O.Box 1568, 3500 BN Utrecht, The Netherlands*

**Summary.** Approximate Bayesian Computation (ABC) methods rely on asymptotic arguments, implying that parameter inference can be systematically biased even when sufficient statistics are available. We propose to construct the ABC accept/reject step from decision theoretic arguments on a suitable auxiliary space. This framework, referred to as ABC\*, fully specifies which test statistics to use, how to combine them, how to set the tolerances and how long to simulate in order to obtain accuracy properties on the auxiliary space. Akin to maximum-likelihood indirect inference, regularity conditions establish when the ABC\* approximation to the posterior density is accurate on the original parameter space in terms of the Kullback-Leibler divergence and the maximum a posteriori point estimate. Fundamentally, escaping asymptotic arguments requires knowledge of the distribution of test statistics, which we obtain through modelling the distribution of summary values, data points on a summary level. Synthetic examples and an application to time series data of influenza A (H3N2) infections in the Netherlands illustrate ABC\* in action.

## 1. Introduction

Approximate Bayesian Computation (ABC) methods have become a popular technique throughout the applied sciences because they can handle posterior densities

$$\pi(\theta|x) \propto \ell(x|\theta)\pi(\theta) \quad (1)$$

that arise under high-dimensional stochastic processes with intractable likelihoods. ABC methods circumvent computations of the likelihood  $\ell(x|\theta)$  by comparing the observed data  $x$  to simulated data  $y$  in terms of many, lower-dimensional summary statistics  $S_k$ . Observed and simulated summary statistics are compared with distances  $d_k(S_k(y), S_k(x)) = S_k(y) -$

$S_k(x)$ ,  $k = 1, \dots, K_S$  and then combined and weighted either under a Mahalanobis approach (Beaumont et al., 2002)

$$\mathbb{1} \left\{ |(d_1, \dots, d_{K_S}) \Sigma^{-1} (d_1, \dots, d_{K_S})^t| \leq c \right\} \quad (2a)$$

or under an intersection approach (Pritchard et al., 1999)

$$\prod_{k=1}^{K_S} \mathbb{1} \left\{ c_k^- \leq d_k \leq c_k^+ \right\} \quad (2b)$$

with a user-defined tolerance  $c \geq 0$  (or  $c_k^- \leq 0, c_k^+ \geq 0$  for all  $k$ ). This 0/1 weight replaces the likelihood term in Monte Carlo algorithms as in the following simple rejection sampler based on (2b):

**standard ABC rejection sampler (ABC-r)**

- 1: **for**  $i = 1 \dots N$  **do**
- 2: Propose  $\theta' \sim \pi$  and simulate  $y' \sim \ell(\cdot | \theta')$ .
- 3: Compute summary statistics  $S_k(y')$ ,  $k = 1, \dots, K_S$ .
- 4: Compute summary errors  $z'_k = d_k(S_k(y'), S_k(x))$  for all  $k$ .
- 5: Accept  $(\theta', z')$  if for all  $k$   $c_k^- \leq z'_k \leq c_k^+$ . Go to line 2.
- 6: **end for**

The ABC likelihood approximation based on the above intersection approach is

$$\ell(x|\theta) \approx \ell_{\text{abc}}(x|\theta) = \int \prod_{k=1}^{K_S} \mathbb{1} \left\{ c_k^- \leq d_k(S_k(y), S_k(x)) \leq c_k^+ \right\} \ell(dy|\theta). \quad (3)$$

Even if the summary statistics are sufficient for  $\theta$ , no ABC theory exists to establish the accuracy of  $\pi_{\text{abc}}(\theta|x) \propto \ell_{\text{abc}}(x|\theta)\pi(\theta)$  in terms of point estimates (such as the maximum a posteriori (MAP) estimate) or distributional properties (such as the Kullback-Leibler (KL) divergence) in the classical, computationally feasible setting that  $c > 0$  or  $c_k^- < c_k^+$ . All available ABC methods invoke asymptotic arguments that involve either the  $c_k^- < c_k^+$  or the number of data points  $n$ . This has led to the notion that ABC is noisy (Fearnhead and Prangle, 2012), despite notable recent advances (Grelaud et al., 2009; Dean et al., 2011; Drovandi et al., 2011; Barnes et al., 2012; Filippi et al., 2013; Marin et al., 2013).

*Example.* Suppose that  $x^{1:n} = (x_1, \dots, x_n)$  are identically and independently  $\mathcal{N}(0, \sigma^2)$  distributed, with  $n = 60$  and unknown  $\sigma^2$ . The true value to be re-estimated is  $\sigma_0^2 = 1$  and we have the prior density  $\pi(\sigma^2) \propto \mathbb{1}\{0.2 < \sigma^2 < 4\}$  so that a simple rejection sampler will suffice. The MAP estimate of the exact posterior density is  $\hat{\theta}^{\text{MAP}} = \frac{1}{n} S^2(x)$ , where  $S^2(x)$  denotes the sum of squares. To employ ABC-r, we decide to simulate data  $y^{1:m} \sim \mathcal{N}(0, \sigma^2)$ , with  $m = 60$  set arbitrarily, compute  $S^2(y^{1:m})$ , consider (arbitrarily) the difference  $z = \frac{1}{m-1} S^2(y) - \frac{1}{n-1} S^2(x)$  as well as (again arbitrarily) the tolerances  $c^+ = 0.4$  and  $c^- = -c^+$ . To evaluate the accuracy of the standard ABC approximation, we also considered  $c^+ = 0.8, 0.2, 0.05$  and ran ABC-r on 4000 pseudo data sets  $x$ . The KL divergence

**Table 1.** Accuracy of parameter estimates with standard ABC and ABC\*

Inference with standard ABC on simulated pseudo data													
	Normal variance				Moving average				Influenza time series				
$d_k$	var( $y$ ) – var( $x$ )				var( $y$ ) – var( $x$ ), cor( $y$ ) – cor( $x$ )				log ratio of sample means <sup>¶</sup>				
$n = m$	60				(150, 149)				(15, 14, 15)				
$c^+, c^- = -c^+$	0.8	0.4	0.2	0.05	0.89	0.71	0.59	0.39	0.18	0.13	0.09	0.03	(0.35, 0.35, 0.03)
$\theta_0$	1				(1, 0.1)				(3.5, 10, 0.08)				
MAP m. s. e.	0.202	0.057	0.012	0.002 <sup>†</sup>	0.27	0.014	0.019	0.017 <sup>†</sup>	1.88 <sup>‡, □</sup>				
KL divergence	4.84	0.41	0.11	0.007 <sup>†</sup>	2.76	0.31	0.15	0.07 <sup>†</sup>	-				
mean acc %	43	22	11	3 <sup>†</sup>	20	10	5	0.5 <sup>†</sup>	5 <sup>‡</sup>				
Inference with ABC* on simulated pseudo data													
	Normal variance				Moving average				Influenza time series				
$T_k$	$\chi^2$				$\chi^2, Z$ ♣				TOST test statistics <sup>♠</sup>				
$n$	60				(150, 149)				(8, 7, 7, 6, 8, 7)				
$m$	108				(297, 278)				variable, e.g. Figure ??A				
$\tau^-$	0.589				(0.705, –0.239)				– $\tau^+$				
$\tau^+$	1.752				(1.432, 0.239)				variable, e.g. Figure ??B				
$\theta_0$	1				(1, 0.1)				(3.5, 10, 0.08)				
MAP m. s. e.	0.002 <sup>†</sup>				0.006 <sup>†</sup>				0.071 <sup>‡, □</sup>				
KL divergence	0.007 <sup>†</sup>				0.07 <sup>†</sup>				-				
mean acc %	13 <sup>†</sup>				5 <sup>†</sup>				14 <sup>‡</sup>				

<sup>†</sup>Computed over 4000 replicate pseudo data sets  $x$ . <sup>‡</sup>Computed over 50 replicate pseudo data sets.  
<sup>¶</sup>The summary statistics are the samples means of the observed and simulated aILI, fdILI and aINC.  
<sup>♠</sup>The summary values are the odd and even subsets of the aILI, fdILI and aINC time series, and one test was used for each set of observed and simulated summary values. <sup>♣</sup>For the configuration that ignores correlations in  $s_k^{1:n_k}$ . <sup>□</sup>Exact posterior density not available. Here, the mean squared error was computed against  $\theta_0$  instead of  $\hat{\theta}^{\text{MAP}}$ .

of  $\pi_{\text{abc}}(\theta|x)$  to  $\pi(\theta|x)$  and the mean square error between the ABC MAP estimate  $\hat{\theta}_{\text{abc}}^{\text{MAP}}$  and  $\hat{\theta}^{\text{MAP}}$  were initially very large and approached zero as predicted (Beaumont et al., 2002), with decreasing tolerances at decreasing acceptance probability (top left in Table 1 and Figure 2D below).

We present a statistical framework that fully specifies the free ABC parameters so that the resulting ABC approximation is accurate in that  $\hat{\theta}_{\text{abc}}^{\text{MAP}} = \hat{\theta}^{\text{MAP}}$  and that the KL divergence of  $\pi_{\text{abc}}(\theta|x)$  to  $\pi(\theta|x)$  is very small. We define the ABC accept/reject step as a statistical decision test with well-understood frequency properties on an empirically validated auxiliary probability space, and then calibrate the free ABC parameters before ABC is run such that the above two approximation criteria are met. This basic procedure is called

ABC\*. Our paper is structured as follows. In Section 2.1, we suggest to construct a suitable auxiliary probability space from independent and approximately sufficient “summary values” whose distribution is relatively simple. These summary values must be identified either by the user or through computational methods and form the interface between the rigorous and automated part of ABC\* with a broad range of inference problems. Section 2.2 develops our notation and the ABC\* approximation on the auxiliary space. Sections 2.3-2.4 present an equivalence hypothesis testing framework under which the ABC approximation emerges as the power function of particular hypothesis test statistics  $T$ , first for the univariate and then for the multivariate case. We then demonstrate in Section 2.5 that the power function can be matched to the likelihood of the summary values on the auxiliary space by calibrating all free ABC parameters. The appropriate test statistics and calibrations can be analytically derived for relatively simple auxiliary probability models on the distribution of the summary values, which explains part of the required regularity conditions. The remaining conditions ensure that indirect inference on the auxiliary space is appropriate for estimating the original parameters of interest, as we outline in Section 2.6. In particular, we identify that the link function between the auxiliary and original parameter space must be bijective and sufficiently regular for ABC\* inference to be accurate, and demonstrate how this can be verified from Monte Carlo output. Finally, ABC\* inference is illustrated at synthetic examples, and its broader applicability is demonstrated on an influenza A (H3N2) virus transmission model.

## 2. Accurate ABC\* parameter inference

### 2.1. Modelling summary values to specify the ABC auxiliary space

We construct a theoretical framework for accurate ABC that is based on modelling distributions of “summary values”, data points on a summary level. We consider multiple sets of summary values,  $k = 1, \dots, K$ , and denote each observed set by  $s_k^{1:n_k} = (s_k^1, \dots, s_k^{n_k})$  and each simulated set by  $s_k^{1:m_k}$ . The  $k' = 1, \dots, K_S$  summary statistics in standard ABC are a function thereof, for example  $S_{k'}(s_k^{1:n_k}) = \frac{1}{n_k} \sum_{i=1}^{n_k} s_k^i$  and  $S_{k'+1}(s_k^{1:n_k}) = \frac{1}{n-1} \sum_{i=1}^n (s_k^i - \bar{s}_k)^2$  (Figure 1). The number of summary values can differ for each  $k$  and between observation and simulation ( $n_k \neq m_k$ ) but is strictly  $> 1$ . We require that summary values can be found such that

- A1** they are sufficient for  $\theta$  and
- A2** their distribution can be modelled so that test statistics  $T_k$  exist and can be calibrated (A2.1-A2.4 below).

Such sets of summary values can be identified in practice as we illustrate in Section 3, although not necessarily in all previous applications of standard ABC. A2 holds, for example, when both the  $s_k^{1:n_k}$  and  $s_k^{1:m_k}$  follow a normal, lognormal,  $\chi^2$  or similar simple distribution. A2 also validates the use of a particular auxiliary probability model based on the available data. The simplest algorithm we consider is:

#### calibrated ABC\* rejection sampler (ABC\*-r)

- 1: **for**  $i = 1 \dots N$  **do**
- 2: Propose  $\theta' \sim \pi$  and simulate data  $y' \sim \ell(\cdot | \theta')$ .

- 3: Extract summary values  $s_k^{1:m_k}(y')$  from  $y'$  for all  $k = 1, \dots, K$ .
- 4: Compute  $z'_k = T_k(s_k^{1:m_k}(y'), s_k^{1:n_k}(x))$  for all  $k$ .
- 5: Accept  $(\theta', z')$  if for all  $k$   $c_k^- \leq z'_k \leq c_k^+$ . Go to line 2.
- 6: **end for**

where the  $T_k$ 's are *specific* hypothesis test statistics, and the  $c_k^-, c_k^+$  are the boundary points of the critical region of these hypothesis tests. The distribution of the summary values determines which  $T_k$  is to be used. The  $T_k$ 's implicitly specify the summary statistics in standard ABC, and generally  $K_S \geq K$ . More complicated Monte Carlo samplers for ABC\* are detailed in the supplementary online material (SOM), section ??.

## 2.2. ABC approximation on the auxiliary space

Figure 1A illustrates our notation to write the ABC\* accept/reject step as a decision problem on the summary space. As the most basic case of A2, we consider  $s_k^{1:m_k}(y) \sim \mathcal{N}(\nu_{\theta k}, \sigma_{\theta k}^2)$ ,  $s_k^{1:n_k}(x) \sim \mathcal{N}(\nu_{xk}, \sigma_{xk}^2)$ . We are interested in testing if the unknown  $\nu_{\theta k}$  and  $\nu_{xk}$  are equal or similar. We refer to the scalar parameters that are subject to testing as the ‘‘summary parameters’’  $\nu_k$ , potentially in the presence of ‘‘hidden parameters’’ such as the  $\sigma^2$ 's above. The summary parameters of the simulated data are denoted by  $\nu_{\theta k}$  to reflect their dependence on  $\theta$ . The summary parameters of the observed data are denoted by  $\nu_{xk}$ . The  $\nu_{xk}$  are unknown. Since we consider the data fixed, these are replaced by maximum likelihood estimates  $\hat{\nu}_{xk}$ . The simulated and observed summary parameters are then compared with a distance function  $\rho_k = \delta_k(\nu_{\theta k}, \hat{\nu}_{xk})$  that takes on values in a subset  $\Delta_k$  of the real line. The point of equality is denoted by  $\rho_k^* = \delta_k(\nu, \nu)$ . This setup defines the link function

$$\mathcal{L} : \Theta \subseteq \mathbb{R}^D \rightarrow \Delta \subseteq \mathbb{R}^K, \quad \theta \rightarrow \rho, \quad \rho = (\rho_1, \dots, \rho_K). \quad (4)$$

Let us first suppose there are no hidden parameters. If A1-A2 hold and if

**A3** the link function  $\mathcal{L}$  is bijective and continuously differentiable,

then the exact posterior density can be written as

$$\pi(\theta|x) \propto \ell(\{s_k^{1:n_k}(x), k = 1, \dots, K\}|\rho) \pi_\rho(\rho) |\partial\mathcal{L}(\theta)|, \quad (5)$$

where  $|\partial\mathcal{L}(\theta)|$  is the absolute value of the determinant of the Jacobian of (4),  $\ell(\{s_k^{1:n_k}(x), k = 1, \dots, K\}|\rho)$  is the likelihood of the summary values under the validated auxiliary probability models, and the prior density  $\pi_\rho$  is induced from  $\pi(\theta)$  through the change of variables. Now, the summary likelihood is known analytically but the  $|\partial\mathcal{L}(\theta)|$  is a priori not known. If  $\mathcal{L}$  was known, then inference could proceed directly via (5) without recursion to the ABC\* algorithm.

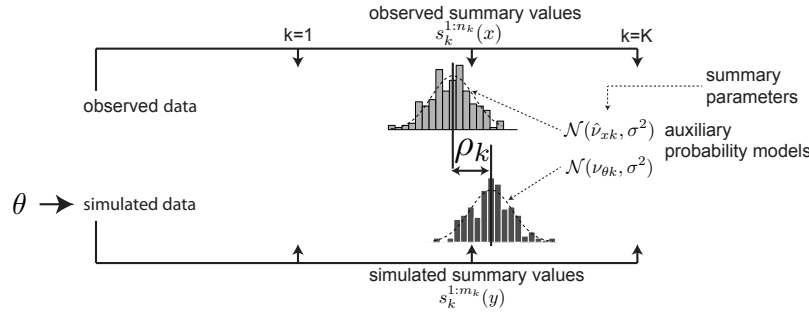
Under the particular auxiliary probability models in A2, the ABC\* approximation to (5) can be written as

$$\pi_{\text{abc}}(\theta|x) \propto P_x(R|\rho) \pi_\rho(\rho) |\partial\mathcal{L}(\theta)|, \quad (6)$$

where either

$$P_x(R|\rho) = \int \mathbf{1} \left\{ |T(s_{1:K}^{1:m}, s_{1:K}^{1:n}(x))| \leq c \right\} F_\rho(ds_{1:K}^{1:m}) \quad (7a)$$

A



B

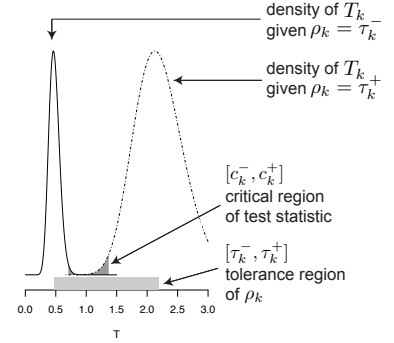


**Fig. 1. Notation for ABC\* parameter inference.** (A) Notation associated with the auxiliary probability models. In the  $\mathcal{N}(\nu_{\theta k}, \sigma_{\theta k}^2)$  basic case,  $\rho_k$  corresponds to the difference in the population means  $\nu_{\theta k} - \nu_{xk}$  and  $\rho_k^*$  equals zero. (B) Notation to construct equivalence tests, illustrated with the probability densities of the equivalence test statistic  $T$ ,  $[\tau_k^-, \tau_k^+]$  and  $[c_k^-, c_k^+]$  in the  $\mathcal{N}(0, \sigma^2)$  example. In this example,  $\rho_k$  corresponds to the ratio  $\nu_{\theta k}/\hat{\nu}_{xk}$  and  $\rho_k^*$  equals one.

in analogy to the Mahalanobis approach (2a) for a multivariate test statistic  $T$  or

$$P_x(R|\rho) = \int \prod_{k=1}^K \mathbb{1} \left\{ c_k^- \leq T_k(s_k^{1:m_k}, s_k^{1:n_k}(x)) \leq c_k^+ \right\} F_\rho(ds_{1:K}^{1:m}) \quad (7b)$$

in analogy to the intersection approach (2b). The subscript  $x$  emphasises that the observed summary values are fixed. The integral evaluates with respect to the distribution of simulated summary values for given  $\rho$  and approximates the summary likelihood. Our key observation is that integrals of the form (7) arise in hypothesis testing theory and are well understood if the distribution of the summary values is sufficiently regular (Wellek, 2003).

Additional hidden parameters of an auxiliary probability model complicate equations (5-6) slightly. Following composite hypothesis testing theory (Lehmann and Romano, 2005), we typically condition  $\ell(\{s_k^{1:n_k}(x), k = 1, \dots, K\}|\rho)$  and  $P_x(R|\rho)$  on additional statistics  $C$ .

### 2.3. Univariate equivalence tests on the auxiliary space

From a Neyman-Pearson *equivalence testing* perspective,  $\rho \rightarrow P_x(R|\rho)$  is the power in *rejecting* the multivariate test statistic  $T = (T_1, \dots, T_K)$  at an error  $\rho$  (hence “R” for reject). We begin with the univariate case. Tests for the point null hypothesis

$$\tilde{H}_{0k} : \nu_{\theta k} = \hat{\nu}_{xk} \quad \text{versus} \quad \tilde{H}_{1k} : \nu_{\theta k} \neq \hat{\nu}_{xk}$$

are designed to declare  $\nu_{\theta k}$  and  $\hat{\nu}_{xk}$  unequal. Because we aim to match the simulated and observed summary values, the ABC\* objective is to declare  $\nu_{\theta k}$  and  $\hat{\nu}_{xk}$  equal. With this objective, Schuirmann (1981) noted that the appropriate hypothesis testing framework is

$$H_{0k} : \rho_k = \delta_k(\nu_{\theta k}, \hat{\nu}_{xk}) \notin [\tau_k^-, \tau_k^+] \quad \text{versus} \quad (8a)$$

$$H_{1k} : \rho_k = \delta_k(\nu_{\theta k}, \hat{\nu}_{xk}) \in [\tau_k^-, \tau_k^+], \quad (8b)$$

for an equivalence region  $[\tau_k^-, \tau_k^+]$  that contains the point of equality  $\rho_k^*$ . Hereafter, we call the  $\tau_k^-$  and  $\tau_k^+$  the “tolerances”. Note that the null and alternative are flipped compared to  $\tilde{H}_{0k}$  and  $\tilde{H}_{1k}$ . This means that *rejecting* an equivalence test for a particular set of simulated summary values  $s_k^{1:m_k}(y')$  implies that the proposed  $\theta'$  in an ABC iteration is *accepted*. The distance function  $\delta_k$  and test statistic  $T_k$  are defined in such a way that the univariate  $P_x(R_k|\rho_k)$  can be evaluated. This is a key difference to standard ABC where  $d_k$  is chosen in an ad-hoc fashion. Wellek (2003) describes many univariate equivalence tests for a variety of distributional assumptions on the summary values. These tests are adapted to the one-sample case because the data  $x$  are considered fixed in ABC\*. The tolerances in standard ABC are the critical region  $[c_k^-, c_k^+]$  of equivalence test statistics, and for given  $\alpha$  obtained as the simultaneous solution to the constraints

$$P_x(c_k^- \leq T_k \leq c_k^+ | \tau_k^-) = \alpha = P_x(c_k^- \leq T_k \leq c_k^+ | \tau_k^+) \quad (9)$$

for continuous  $T_k$  (see also Figure 1B). The size of the univariate test,  $\sup_{\rho_k \in H_{0k}} P_x(c_k^- \leq T_k \leq c_k^+ | \rho_k)$ , is then equal to  $\alpha$  and limits the probability to falsely accept  $\rho_k$  at any ABC\* iteration. The power of the test gives the probability to correctly accept  $\rho_k$  at any ABC\* iteration.

*Example.* Consider the basic  $\mathcal{N}(0, \sigma^2)$  example where the single parameter  $\sigma^2$  is to be estimated. We will therefore only need one test statistic ( $K = 1$ , and we drop  $k$ ). The  $n = 60$  data points act as the observed summary values, the link function is the identity, and we let  $m \geq n$ . Since the summary values are normally distributed, we choose the scaled  $\chi^2$  test and set  $\rho = \delta(\sigma^2, \hat{\sigma}_x^2) = \sigma^2 / \hat{\sigma}_x^2 \in (0, \infty)$  where  $\hat{\sigma}_x^2$  is the maximum likelihood estimate  $\frac{1}{n} S^2(x)$  (Wellek, 2003). The point of equality is  $\rho^* = 1$ . We consider  $\tau^- \leq \rho^* \leq \tau^+$  and test  $H_0: \rho \notin [\tau^-, \tau^+]$  versus  $H_1: \rho \in [\tau^-, \tau^+]$  with the test statistic

$$T(y) = \frac{S^2(y)}{S^2(x)} = \frac{\sigma^2}{\hat{\sigma}_x^2} \frac{1}{n} \sum_{i=1}^m \left( \frac{y_i - \bar{y}}{\sigma} \right)^2. \quad (10)$$

$\frac{n}{\rho} T$  follows a  $\chi^2$ -distribution with  $m - 1$  degrees of freedom,  $F_{\chi_{m-1}^2}$ . We set  $\alpha = 0.01$ . The size- $\alpha$  ABC\* acceptance region  $[c^-, c^+]$  is the solution of the equations

$$\begin{aligned} \alpha &= F_{\chi_{m-1}^2}(nc^+/\tau^+) - F_{\chi_{m-1}^2}(nc^-/\tau^+) \\ \alpha &= F_{\chi_{m-1}^2}(nc^+/\tau^-) - F_{\chi_{m-1}^2}(nc^-/\tau^-), \end{aligned} \quad (11)$$

as illustrated in Figure 1B. Having solved for  $c^-$  and  $c^+$ , the power is

$$P_x(c^- \leq T \leq c^+ | \rho) = F_{\chi_{m-1}^2}(nc^+/\rho) - F_{\chi_{m-1}^2}(nc^-/\rho). \quad (12)$$

This is the probability to accept a single ABC\* iteration, conditional on the underlying population level variance of the simulated summary values being a multiple  $\rho$  of  $\hat{\sigma}_x^2$ . It is thus possible to quantify the behaviour of the ABC\* accept/reject step exactly for the particular distance function and test statistic above.

We focus on  $\tau^- < \tau^+$  because for  $\tau^- = 1 = \tau^+$  power is too small in practice,  $P_x(c^- \leq T \leq c^+ | \rho = 1) = \alpha = 0.01$ . Then, the power function is larger or equal than  $\alpha$  and maximised

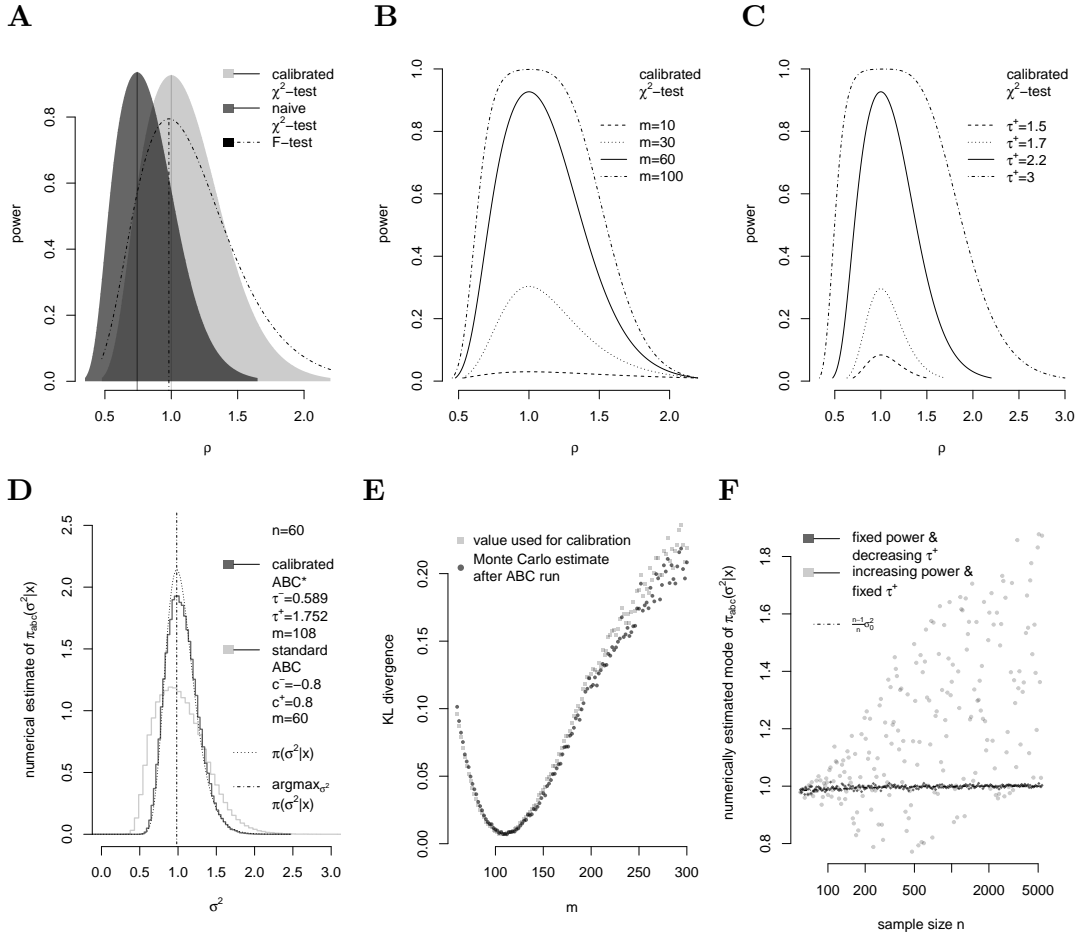


**Fig. 2.** Power function of the  $\chi^2$  equivalence test statistic and ABC\* inference of  $\sigma^2$ . (A) Power function of the univariate  $\chi^2$  test statistic for two different tolerance regions. For  $n = m = 60$  and  $\alpha = 0.01$ , we considered first  $[\tau^-, \tau^+] = [1 - 0.65, 1 + 0.65]$  which lead to  $[c^-, c^+] \approx [0.509, 1.009]$  as the solution to (11). The power function (dark gray) has a unimodal shape and maximises at  $\rho^{\max} < \rho^* = 1$ . Next, we fixed  $\tau^+ = 2.2$  and calibrated  $\tau^- = 0.477$  such that the power function maximises at  $\rho^* = 1$  (light gray). In this case,  $[c^-, c^+] = [0.704, 1.368]$ . Note that, if the observed summary values were considered random even though they are fixed in practice, then  $T/\rho$  would follow an  $\mathcal{F}$  distribution with  $n - 1, m - 1$  degrees of freedom (Wang, 1997) and the power function would differ from (12) (dash-dot for same  $[c^-, c^+]$ ). (B) Power of the  $\chi^2$  test as  $m = n$  increases for fixed  $\tau^+ = 2.2$  and calibrated  $\tau^-$  such that  $\rho^{\max} = \rho^*$ . (C) Power of the  $\chi^2$  test as  $\tau^+$  increases for fixed  $m = n = 60$  and calibrated  $\tau^-$  such that  $\rho^{\max} = \rho^*$ . (D) We then estimated  $\sigma^2$  in  $\mathcal{N}(0, \sigma^2)$  under the prior density specified in the main text with ABC\*. (dotted) Exact posterior density  $\pi(\sigma^2|x)$  and (dash-dot) the MAP estimate of  $\sigma^2$  under  $\pi(\sigma^2|x)$ . (dark gray) Histogram of the ABC approximation  $\pi_{\text{abc}}(\sigma^2|x)$  for calibrated  $\tau^-, \tau^+, m$ . (light gray) Histogram of  $\pi_{\text{abc}}(\sigma^2|x)$  for the standard ABC approximation used in the introduction, with  $z = S^2(y) - S^2(x)$ ,  $[c^-, c^+] = [-0.8, 0.8]$  and  $m = 60$ . The ABC\* approximation obtained with ABC\*-r has a KL divergence of 0.007 and an acceptance probability of 12%, while ABC-r reaches similar accuracy for  $[c^-, c^+] = [-0.05, 0.05]$  at 3% acceptance probability (top and bottom left in Table 1). (E) KL divergence for increasing  $m$  as used for calibrations before ABC was run (light gray) and as estimated from Monte Carlo output after ABC was run (dark gray). (F) To assess numerical robustness, we compared ABC\* for increasing  $n = m$  when  $\tau^+ = 2.2$  was fixed throughout to the case where  $\tau^+$  was calibrated. In both cases, we numerically estimated the mode of  $\pi_{\text{abc}}(\theta|x)$  as a function of  $n$ . Calibration of  $\tau^+$  leads to numerically stable estimates of  $\hat{\theta}_{\text{abc}}^{\text{MAP}}$ .



somewhere in  $[\tau^-, \tau^+]$ , see Figure 2A. Calibrating the values  $\tau^-, \tau^+$ , e.g. to 0.477 and 2.2, we can ensure that the value of  $\rho$  with largest power coincides with  $\rho^*$ . Figure 2B illustrates that the power increases with  $m$ . Figure 2C illustrates that the power also increases for increasing  $\tau^+$ . Here,  $\tau^-$  was calibrated so that the largest power coincides with  $\rho^*$ .

A few points are worth emphasising. In the interesting case  $\tau_k^- < \rho_k^* < \tau_k^+$ , the power function of two-sided equivalence hypothesis test statistics  $\rho_k \rightarrow P_x(R_k | \rho_k)$  has a unimodal shape within  $[\tau_k^-, \tau_k^+]$ . We will make extensive use of this property, which does not hold for one-sided equivalence hypothesis tests or point null hypothesis tests. This limits all tests of interest to those of the form (8). Moreover, two-sample equivalence tests have different power functions, which limits interest further to one-sample tests of the form (8) for fixed data  $x$  (Figure 2A). Finally, equation (11) implies that the calibrated  $[c^-, c^+]$  for which power is maximised at  $\rho^* = 1$  do not necessarily include the point  $T = 1$ . This is especially so when  $m \gg n$ . The correct critical regions used in ABC\* are not necessarily what might be naively expected at first sight.

#### 2.4. Multivariate equivalence tests on the auxiliary space

*Composite approach.* As we aim for a bijective link function, we typically need to handle several tests simultaneously and need to characterise the multivariate  $\rho \rightarrow P_x(R | \rho)$ . In the equivalence testing framework, sufficiently regular multivariate tests are straightforward to construct from disparate univariate tests. For all  $k = 1, \dots, K$ , suppose the distribution of summary values is such that

- A2.1** there are level- $\alpha$  test statistics  $T_k$  with rejection regions  $R_k = [c_k^-, c_k^+]$  for univariate equivalence hypotheses (8) with a unimodal power function  $\rho_k \rightarrow P_x(R_k | \rho_k)$ ,
- A4** the family of distributions induced by  $T_k$  is independent of  $\rho_j$  for  $j \neq k$ .

Then, as shown by Berger and Hsu (1996), the multivariate statistic  $T = (T_1, \dots, T_K)$  with the hypercube rejection region  $R = \bigcap_{k=1}^K [c_k^-, c_k^+]$  is level- $\alpha$  for

$$H_0 = \bigcup_{k=1}^K H_{0k} \text{ versus } H_1 = \bigcap_{k=1}^K H_{1k}. \quad (13)$$

The power of the multivariate  $T$  has a unique mode  $\rho^{\max}$  and decreases monotonically in each direction from  $\rho^{\max}$ , which follows from A2.1 because A4 implies  $P_x(R | \rho) = \prod_{k=1}^K P_x(R_k | \rho) = \prod_{k=1}^K P_x(R_k | \rho_k)$ . The resulting ABC accept/reject step is exactly (2b), so we can interpret (2b) as the outcome of a composite testing approach in which all tests are assumed to be independent. No downwards adjustment on the level of the individual tests is necessary to obtain a multivariate level- $\alpha$  equivalence test statistic. Based on the argument in Figure ??, we fix  $\alpha = 0.01$ . The main appeal of the composite approach is that we can combine different univariate tests in a flexible manner. A2.1 is met when the distribution of summary values is continuous in  $\rho$  and strictly totally positive of order 3 (STP<sub>3</sub>) (Wellek, 2003, p369), but also in other cases. The main limitation is A4, which is clear by considering the equivalent statement to the summary likelihood,

- A5**  $\ell(\{s_k^{1:n_k}(x), k = 1, \dots, K\} | \rho) = \prod_{k=1}^K \ell(s_k^{1:n_k}(x) | \rho_k)$ .

*Mahalanobis approach.* The alternative Mahalanobis approach (7a) is highly used in ABC. It corresponds to a multivariate equivalence test of  $K$  population means of  $K$  sets of multivariate Gaussian summary values (Wellek, 2003, p221ff). So it is only applicable in this basic case. There is only one scalar tolerance parameter  $\tau > 0$ ,  $\tau^- = -\tau$ ,  $n_k = n$ ,  $m_k = m$  and the resulting critical region is described by  $c > 0$  as in (7a). A2.1 is not met exactly because the test is not exactly level- $\alpha$  but alternatives exist at least in the univariate case (Berger and Hsu, 1996). Importantly, the summary values can be correlated in this case (A4-A5 not required).

## 2.5. Calibration

*Composite approach.* Our next observation is that the free parameters of the equivalence tests can be calibrated such that  $P_x(R|\rho)$  is close to  $\ell(\{s_1^{1:n_1}(x), \dots, s_K^{1:n_K}(x)\} | \rho)$  on the auxiliary space. For each  $k$ , we further assume

**A2.2**  $P(R_k|\rho_k)$  is continuous in  $\tau_k^-$  and  $\tau_k^+$

**A2.3**  $\operatorname{argmax}_{\rho_k} P(R_k|\rho_k)$  shifts to the right (left) when  $\tau_k^-$  decreases (increases)

**A2.4** the equivalence test induced by  $T_k$  is consistent,

and proceed in three hierarchical steps. At the lowest level, we calibrate  $\tau_k^-$  for given  $\tau_k^+$  and  $m_k$  such that the modes of the univariate  $\rho_k \rightarrow P_x(R_k|\rho_k)$  and  $\rho_k \rightarrow \ell(s_k^{1:n_k}(x)|\rho_k)$  coincide. We discussed this possibility already on the  $\mathcal{N}(0, \sigma^2)$  example (Figure 2A). Next, we calibrate  $\tau_k^+$  for given  $m_k$  for numerical stability. This will include repeat calls to the first calibration step. Estimating the mode of  $\rho_k \rightarrow P_x(R_k|\rho_k)$  from Monte Carlo output is numerically more stable when this function is not too flat around  $\rho_k^*$ . Power functions are flat if they are close to zero *or* one for all  $\rho_k$ . We saw in Figure 2C that the flatness around  $\rho_k^*$  can be adjusted by changing the width of the tolerance region, and this is why we calibrate  $\tau_k^+$ . At the top level, we calibrate  $m_k$  such that the KL divergence of  $P_x(R_k|\rho_k)$  to  $\ell(s_k^{1:n_k}(x)|\rho_k)$  is minimised. This will involve calls to the first two calibration steps. As power concentrates with increasing  $m_k$  under A2.4, we are able to offset the broadening effect of the ABC tolerances by choosing  $m_k > n_k$ . Using A4-A5, the multi-dimensional end-product is a numerically stable ABC approximation that minimises its KL divergence to the exact summary likelihood, subject to the constraint that their modes coincide. Full details are found in SOM ?? and calibration routines are available from <https://github.com/olli0601/abc.star>.

*Mahalanobis approach.* If the assumptions on the  $s_k^{1:n_k}$  are met so that the test is applicable, calibrations proceed as for a single  $k$  under the composite approach. A4-A5 are not required and A2.2-A2.4 are met.

## 2.6. ABC\* parameter inference

The remaining question is when these calibrations on the auxiliary parameter space improve the accuracy of the ABC\* approximation  $\pi_{\text{abc}}(\theta|x)$  to the exact posterior density  $\pi(\theta|x)$ . We need to limit considerations to the case where a model can explain the data in terms of the summary values. To this end, we require that the support of the prior density  $\pi_\rho$

must extend beyond the tolerance region. In particular, it must include the point of equality so that there is  $\hat{\theta}$  such that  $\mathcal{L}(\hat{\theta}) = \rho^*$ . The basis for indirect inference is that maximum likelihood estimators are invariant under parameter transformation (Gouriéroux et al., 1993). In ABC\*, the rationale for calibrating with respect to the KL divergence is as well that the KL divergence between two densities is invariant under parameter transformation.

**THEOREM 1. (Minimal KL divergence)** *Suppose that the prior density on the auxiliary space is flat. (i) For the composite  $T = (T_1, \dots, T_K)$ , suppose that summary values can be constructed such that A1-A5 hold. Calibrate  $\tau_k^-, \tau_k^+, m_k$ . Then*

$$\text{KL}(\pi(\theta|x) \parallel \pi_{\text{abc}}(\theta|x)) = \sum_{k=1}^K \varepsilon_k, \quad (14)$$

where  $\varepsilon_k = \text{KL}(\ell(s_k^{1:n_k} | \rho_k(x)) \parallel P_x(R_k | \rho_k))$ . (ii) For the Mahalanobis approach, suppose that the summary values are multivariate normal and that A1, A3 hold. Calibrate  $\tau, m$ . Then  $\text{KL}(\pi(\theta|x) \parallel \pi_{\text{abc}}(\theta|x)) = \text{KL}(\ell(\{s_1^{1:n_k}(x)\}_{1:K} | \rho) \parallel P_x(R|\rho)) = \varepsilon$ .

The proof is given in Appendix ???. We can also control the accuracy of the MAP point estimate of  $\pi_{\text{abc}}(\theta|x)$ . Considering the maximum likelihood estimate  $\hat{\theta}^{\text{MLE}} = \text{argmax}_{\theta} \ell(x|\theta)$ , we have  $\mathcal{L}(\hat{\theta}^{\text{MLE}}) = \text{argmax}_{\rho} \ell(x|\rho)$ . With the calibrations in Section 2.5, we also have  $\mathcal{L}(\hat{\theta}^{\text{MLE}}) = \rho^* = \text{argmax}_{\rho} P_x(R|\rho)$ . With A3, we obtain  $\hat{\theta}^{\text{MLE}} = \text{argmax}_{\theta} P_x(R|\theta) = \hat{\theta}_{\text{abc}}^{\text{MLE}}$ . To extend this fact to the MAP estimate of  $\pi_{\text{abc}}(\theta|x) \propto P_x(R|\rho) \pi_{\rho}(\rho) |\partial \mathcal{L}(\theta)|$ , we note that the influence of the typically non-constant  $|\partial \mathcal{L}(\theta)|$  can be mitigated if  $P_x(R|\rho)$  peaks on a small area around  $\rho^*$ . We require that

**A6**  $\pi_{\text{abc}}(\rho|x)$  decays faster around  $\rho^*$  than  $|\partial \mathcal{L}(\theta)|$  increases around  $\theta_x = \mathcal{L}^{-1}(\rho^*)$  and in this case we say that the *data control the change of variables*.

**THEOREM 2. (Exact MAP estimate)** *Suppose that the prior density on the auxiliary space does not change the location of  $\text{argmax}_{\rho} P_x(R|\rho)$ . (i) For the composite  $T = (T_1, \dots, T_K)$ , suppose that summary values can be constructed such that A1-A5 hold and calibrate  $\tau_k^-, \tau_k^+, m_k$ . (ii) For the Mahalanobis approach, suppose that the summary values are multivariate normal and that A1, A3 hold, and calibrate  $\tau, m$ . In both cases,*

$$\hat{\theta}_{\text{abc}}^{\text{MAP}} = \text{argmax}_{\theta} \pi_{\text{abc}}(\theta|x) = \text{argmax}_{\theta} \pi(\theta|x). \quad (15)$$

*Example.* We consider one more time the basic  $\mathcal{N}(0, \sigma^2)$  example, for which we already constructed the  $\chi^2$  test statistic and the critical region  $[c^-, c^+]$  appropriate for testing dispersion equivalence of normally distributed summary values (A2.1 met). These  $T$  and  $[c^-, c^+]$  are used to construct the ABC\* algorithm for given  $n$  and fixed  $\alpha = 0.01$ . Inspecting (12), we see that A2.2-A2.4 are met. A1, A3, A6 are not needed because the data can be directly taken as the summary values. A4-A5 are not needed in this univariate example. We can therefore apply the calibrations described in Section 2.5. For these calibrations, we need to know the likelihood density on  $\rho$ -space, which follows from  $S^2(x)/\sigma^2 \sim \chi_{n-1}^2$ .

We calibrated the free ABC parameters to  $m = 108$ ,  $[\tau^-, \tau^+] = [0.589, 1.752]$  and  $[c^-, c^+] = [1.41, 2.22]$  before ABC was run. The point  $T = 1$  is not included in the calibrated  $[c^-, c^+]$ . For the purpose of illustration, we considered a pseudo data set  $x$  such that  $\hat{\sigma}_x^2$  was exactly  $\theta_0 = 1$  (except for Figure 2E-F). We then ran ABC\* for the flat prior distribution  $\pi(\sigma^2) = \mathcal{U}(0.2, 4)$ . As predicted by Theorem 2,  $\hat{\theta}_{\text{abc}}^{\text{MAP}}$  is very close to the mode of the posterior density (Figure 2D), with a mean absolute error of 0.002 over 4000 pseudo data sets  $x$  (bottom left in Table 1). After the ABC run, we estimated the KL divergence of  $\pi_{\text{abc}}(\sigma^2|x)$  to the posterior density from Monte Carlo output at 0.007. Figure 2E shows that the KL divergence is indeed minimised for values of  $m$  that are larger than  $n$ . Increasing  $m$  beyond 108,  $\pi_{\text{abc}}(\sigma^2|x)$  concentrates more tightly at  $\frac{1}{n}S^2(x)$  than  $\pi(\sigma^2|x)$ .

Finally, to illustrate the importance of calibrating  $\tau^+$ , we considered observed and simulated data sets that increase in size from  $n = m = 60$  to 5000. First, we fixed  $\tau^+ = 2.2$  throughout (and hence also  $\tau^-$ ), so that power increases with size and  $P_x(c^- \leq T \leq c^+|\rho)$  becomes more flat around  $\rho^*$  (Figure 2C). Second, we calibrated  $\tau^+$  (and hence also  $\tau^-$ ) for every  $m$  as described in Section 2.5 (Figure ??). We ran ABC\* as above for increasing  $n$  and both sets of tolerance values. In each case, we estimated the mode of  $\pi_{\text{abc}}(\theta|x)$  from Monte Carlo output. For fixed  $\tau^+ = 2.2$ , the Monte Carlo estimate of  $\hat{\theta}_{\text{abc}}^{\text{MAP}}$  can be any value such that the corresponding  $\rho$  lies on the flat part of  $P_x(c^- \leq T \leq c^+|\rho)$ . By contrast, for calibrated  $\tau^+$ , the Monte Carlo estimate of  $\hat{\theta}_{\text{abc}}^{\text{MAP}}$  remains close to  $\hat{\theta}^{\text{MAP}}$  (Figure 2F).

### 3. Application to time series dynamics

#### 3.1. Synthetic moving average time series

The challenge in applying ABC\* to complex inferential problems lies in identifying and modelling summary values such that A1-A3 are met. We illustrate with data generated by a moving average process of order one (MA(1)) for which consecutive observations in time are correlated and sufficient statistics other than the full data cannot be found. Let  $x_t = u_t + a_0 u_{t-1}$  where  $u_t \sim \mathcal{N}(0, \sigma_0^2)$  for  $t = 1, \dots, n$  and  $a_0 = 0.1$ ,  $\sigma_0^2 = 1$ ,  $n = 150$ . The time series has variance  $\nu_{x1} = (1 + a_0^2)\sigma_0^2$  and autocorrelation  $\nu_{x2} = a_0/(1 + a_0^2)$ . We exploit this relationship to re-estimate  $\theta = (a, \sigma^2)$ . Tests for the equivalence of the auxiliary variance and autocorrelation are available (SOM ??) but require independent normally distributed data points. To proceed, we defined summary values as thinned subsets of the time series, e. g.  $s_{1a}^i = x^{2i-1}$  and  $s_{1b}^i = x^{2i}$ ,  $i = 1, \dots, n/2$ ; or simply ignored autocorrelations in the summary values, e. g.  $s_1^i = x^i$ ,  $i = 1, \dots, n$  for the variance test (see also Figure ??). Given these tests, we have  $\mathcal{L}: \theta = (a, \sigma^2) \rightarrow \rho = (\rho_1, \rho_2)$  with

$$\begin{aligned} \rho_1 &= (1 + a^2)\sigma^2/\hat{\nu}_{x1} \\ \rho_2 &= \text{atanh}(a/(1 + a^2)) - \text{atanh}(\hat{\nu}_{x2}), \end{aligned} \tag{16}$$

which is bijective. Its Jacobian  $\partial\mathcal{L}$  is

$$\begin{pmatrix} \frac{\partial\mathcal{L}_1}{\partial a} & \frac{\partial\mathcal{L}_1}{\partial\sigma^2} \\ \frac{\partial\mathcal{L}_2}{\partial a} & \frac{\partial\mathcal{L}_2}{\partial\sigma^2} \end{pmatrix} = \begin{pmatrix} 2a\sigma^2/\hat{\nu}_{x1} & (1 + a^2)/\hat{\nu}_{x1} \\ (1 - a^2)/(1 + a^2 + a^4) & 0 \end{pmatrix},$$

and the rate of change is  $|\det \partial\mathcal{L}| = (1 - a^4)/((1 + a^2 + a^4)\hat{\nu}_{x1})$  (Figure ??A). The points of equality are  $\rho_1^* = 1$  and  $\rho_2^* = 0$ . In more complicated applications,  $\mathcal{L}$  is unknown. The

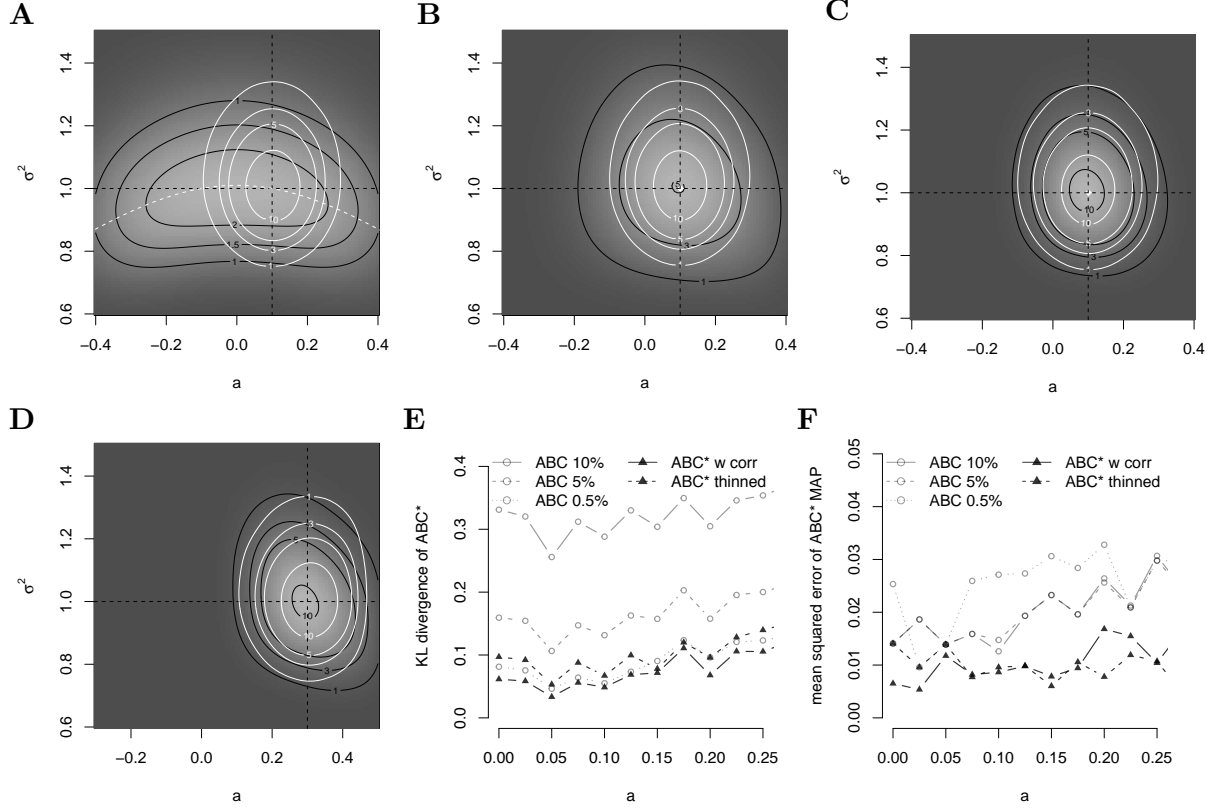


**Fig. 3.** ABC\* inference for the MA(1) model. We considered the prior density  $\pi(\theta)$  induced by a uniform prior on  $\rho = (\rho_1, \rho_2)$  and  $a_0 = 0.1$ ,  $\sigma_0^2 = 1$ . The exact posterior density (white contours) was estimated with MCMC. (A) 2D histogram of the estimated ABC\* posterior density, using only the dispersion test and ignoring autocorrelations. The ABC\* approximation aligns around the level set. (B) 2D histogram of the estimated ABC\* posterior density, using the dispersion and correlation test on the subsets  $s_{1a}$  and  $s_{2a}$  defined in the main text. The ABC\* approximation is broader than  $\pi(\theta|x_{1:n})$ . (C) 2D histogram of the estimated ABC\* posterior density, using two dispersion and three correlation tests so that A1, A3 are met. The ABC\* approximation is very close to  $\pi(\theta|x)$ . (D) Same as (C) but for  $a_0 = 0.3$ . (E) Comparison of the KL divergence of  $\pi_{\text{abc}}(\theta|x_{1:n})$  to  $\pi(\theta|x_{1:n})$  for ABC-r with decreasing acceptance probabilities (gray) and ABC\*-r for the configuration in subfigure C and the case where autocorrelations in the  $s_1$  and  $s_2$  are ignored. ABC-r must be run at very small acceptance probabilities of 0.5% in order to match the accuracy in KL divergence of ABC\*-r, which had a 5% acceptance probability. (F) Same as Figure 3C for the mean squared error between  $\hat{\theta}_{\text{abc}}^{\text{MAP}}$  and  $\hat{\theta}^{\text{MAP}}$ .

MA(1) example with  $\mathcal{L}$  known serves to illustrate the influence of  $\mathcal{L}$  on  $\pi_{\text{abc}}(\theta|x_{1:n})$ . For this purpose, we also constructed from (16) a prior density  $\pi(\theta)$  that is uniform on the auxiliary space (SOM ??). This prior was used throughout. To assess the ABC\* approximation, we estimated the exact  $\pi(\theta|x_{1:n})$  with an MCMC sampler using  $2 \times 10^6$  iterations (white contours in Figure 3, SOM ??). For the purpose of illustration, we chose  $x$  such that  $\hat{\theta}^{\text{MAP}}$  of  $\pi(\theta|x_{1:n})$  was exactly  $\theta_0 = (a_0, \sigma_0^2)$ .

First, we used *the dispersion test only* on the  $s_1$  defined above and *ignored autocorrela-*

tions in the time series ( $n_1 = 150$ ; A1-A3 not met; A4-A5 not required). We calibrated in analogy to the  $\mathcal{N}(0, \sigma^2)$  example and then ran ABC\*-r for  $2 \times 10^6$  iterations. The estimated  $\pi_{\text{abc}}(\theta|x_{1:n})$  aligned around the level set  $\mathcal{L}_1^{-1}(\rho_1^*) = \{a, \sigma^2 | \sigma^2(1+a^2) = \hat{\nu}_{x_1}\}$  because A3 was not met, and was not accurate (Figure 3A; KL divergence was very large, 1.08). Second, we used the dispersion and the autocorrelation tests under the composite testing approach on *thinned subsets* of  $x_{1:n}$ , the  $s_{1a}$  defined above and  $s_{2a} = (x_1, x_2), (x_4, x_5), \dots$  ( $n_1 = 75$ ,  $n_2 = 49$ ; A1 not met; A2-A5 met). We calibrated as described in Section 2.5. The resulting link function is bijective. The ABC\* posterior density resolved the identifiability issue but was still broader than  $\pi(\theta|x_{1:n})$  (Figure 3B; KL divergence was large, 0.41). Third, we combined two dispersion tests using the  $s_{1a}^i$  and  $s_{1b}^i$  and three correlation tests (see SOM ??) so that *the full time series data was used* (A1-A3 met; A4-A5 not met). The resulting ABC\* accuracy error in the MAP estimate and the KL divergence were small (0.005 and 0.07 respectively) at an acceptance probability of 5% for different values of  $a_0$  (Figure 3C-E). Interestingly, we obtained very similar accuracy when the two sets of summary values  $s_1$  and  $s_2 = (x_1, x_2), (x_2, x_3), \dots$  were used and autocorrelations were simply ignored (A1, A3-A5 met; A2 not met; bottom centre in Table 1 and Figure 3E; KL divergence was small, 0.07).

We also compared the calibrated ABC\* posterior density to a standard ABC approximation. Many choices for the free ABC parameters are conceivable. We considered the difference in the variances and autocorrelations, set  $c_k^- = -c_k^+$  and chose  $c_k^+$  such that the final acceptance probability was 10%, 5% and as small as possible before Monte Carlo error became noticeable, 0.5% after  $2 \times 10^6$  iterations (Figure ??E). The standard ABC MAP estimate was not accurate and the KL divergence was comparable to that of ABC\* at an acceptance probability of 0.05%, which corresponds to a 10-fold loss in efficiency relative to ABC\* (top centre in Table 1 and Figure 3E).

To summarise, we applied ABC\* to a time series example that is complex enough so that no sufficient summary statistics exist, but still simple enough so that the link function is known analytically and  $\pi(\theta|x_{1:n})$  can be computed. The model parameters  $\theta = (a, \sigma^2)$  are only identifiable with ABC\* when the link function is bijective. It was most important to meet A3. Thinning the time series lead to irreversible loss of information, and it was important to meet A1. Simply ignoring the autocorrelations in  $s_1$  and  $s_2$  lead to comparable results as with the most complex subsetting procedure, and both configurations gave overall better accuracy results than standard ABC at a 10-fold higher acceptance probability. It was least important to meet the independence assumption in A2. Nonetheless, A2 cannot be neglected entirely because the predicted KL divergence based on the calibrations was  $\approx 10^{-3}$  and substantially smaller than the actual KL divergence of the ABC\* approximation.

### 3.2. Influenza A (H3N2) time series data

To illustrate that ABC\* can be applied to complex inference problems, we consider weekly influenza-like-illness sentinel surveillance data that is attributable to the influenza A (H3N2) virus in the Netherlands (Figure 4). The magnitude, variation and correlation in annual attack rates (cumulative incidence per winter season divided by population size) are characteristic features of seasonal H3N2 dynamics (Ratmann et al., 2012). We considered annual attack rates of the reported ILI time series data (aILI), their first-order differences (fdILI) and independent estimates of annual population-level attack rates in H3N2 seasons (aINC).

The aILI, fdILI and aINC of the simulated data are biennial, and those for the empirical data are weakly so (Figure 4). We formed two sets of summary values for each of the aILI, fdILI and aINC by retaining odd and even values respectively (i. e.  $K = 6$ ). Stationarity, independence and normality of these summary values could not be rejected (Figure 4). We therefore chose the TOSTs from (Wellek, 2003) to test for location equivalence (A2 met).

We aim to fit an epidemiological compartment model which describes H3N2's disease dynamics in a population stratified into susceptible (S), infected but not yet infectious (E), infectious ( $I_1$  and  $I_2$ ) and immune (R) individuals across two large spatial areas. The transmission rate  $\beta_t^\downarrow = \beta(1 + \varphi^\downarrow \sin(2\pi(t - t^\downarrow)))$  is seasonally forced in the sink population that represents the Netherlands (indicated by  $\downarrow$ ), and only weakly so in the source population (indicated by  $\circ$ ) where the virus persists and from where the winter epidemics in the sink population are seeded.  $1/\gamma$  is the average duration in years of host immunity to the virus. All parameters and accompanying prior distributions are described in Table ??, and the model is easily simulated from Markov transition probabilities derived from the deterministic ordinary differential equations

$$\begin{aligned}
 \frac{dS^\downarrow}{dt} &= \mu^\downarrow(N^\downarrow - S^\downarrow) - \beta_t^\downarrow \frac{S^\downarrow}{N^\downarrow} (I_1^\downarrow + I_2^\downarrow + M^\downarrow) + \gamma R^\downarrow \\
 \frac{dE^\downarrow}{dt} &= \beta_t^\downarrow \frac{S^\downarrow}{N^\downarrow} (I_1^\downarrow + I_2^\downarrow + M^\downarrow) - (\mu^\downarrow + \phi) E^\downarrow \\
 \frac{dI_1^\downarrow}{dt} &= \phi E^\downarrow - (\mu^\downarrow + 2\nu) I_1^\downarrow \\
 \frac{dI_2^\downarrow}{dt} &= 2\nu I_1^\downarrow - (\mu^\downarrow + 2\nu) I_2^\downarrow \\
 \frac{dR^\downarrow}{dt} &= 2\nu I_2^\downarrow - (\mu^\downarrow + \gamma) R^\downarrow
 \end{aligned} \tag{17}$$

where  $N^\downarrow = S^\downarrow + E^\downarrow + I_1^\downarrow + I_2^\downarrow + R^\downarrow$ , and identically for the source population with  $\varphi^\circ \ll \varphi^\downarrow$  (equations not shown). Infected travellers from the source population are defined by  $M^\downarrow = m^\downarrow(I_1^\circ + I_2^\circ)/N^\circ$  where the number of travelling individuals  $m^\downarrow$  is a model parameter; see Ratmann et al. (2012) for details. To fit (17) to the ILI time series, we used a Poisson observation model of new weekly ILI cases with mean  $\omega I_1^{\downarrow+}$ , where  $I_1^{\downarrow+}$  is the number of newly infected individuals in the sink population per week and  $\omega$  is the reporting rate.

The key parameters of interest to us are  $\theta = (R_0, 1/\gamma, \omega)$ , where the baseline transmission rate  $\beta$  is re-parameterised into the basic reproductive number  $R_0$  at disease equilibrium for ease of interpretation. We used the broad prior densities  $R_0 \sim \mathcal{U}(1, 8)$ ,  $1/\gamma \sim \mathcal{U}(2, 30)$ ,  $\omega \sim \mathcal{U}(0, 1)$  throughout. The  $\theta$  are unidentifiable under the exact likelihood of the ILI time series due to loss of host immunity to the virus after infection (Truscott et al., 2011). In particular,  $R_0$  and  $1/\gamma$  are strongly positively correlated over a large range of values.

We hypothesised that the  $\theta$  are identifiable from ILI time series data *and annual H3N2 incidence attack rates* (Cox and Subbarao, 2000, between 10 to 20% for the Northern Hemisphere) with ABC techniques, because the latter add absolute information on the burden of seasonal infection. Pseudo data sets  $x$  (comprising both types of data) were generated for several realistic parameter combinations, e. g.  $\theta_0 = (3.5, 10, 0.08)$  in Figure 4. The aILI and fdILI were computed from the ILI cases simulated under the Poisson observation model, and aINC was directly computed from simulated incidence. Previously, we used a Markov Chain

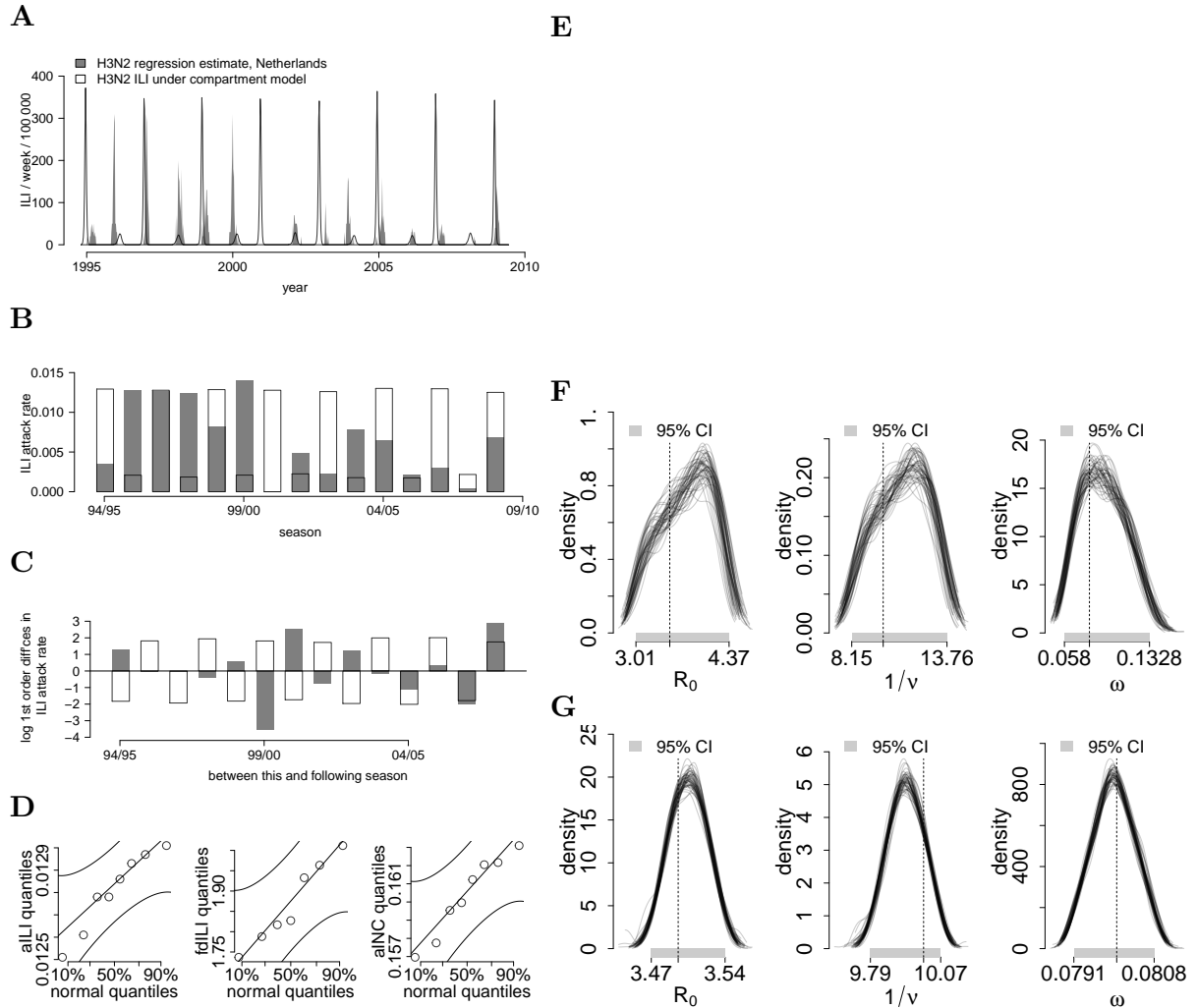


**Fig. 4. Summary values for influenza A (H3N2) time series data and ABC\* inference**  
 (A) Weekly ILI time series that is attributable to influenza A (H3N3) virus in the Netherlands under a regression model (gray), plus simulated incidence data under model (17) (black lines) with parameters  $R_0 = 3.5$ ,  $1/\phi = 0.9$ ,  $1/\nu = 1.8$ ,  $1/\gamma = 10$ ,  $\omega = 0.08$ ,  $N^\circ = 2 \times 10^8$ ,  $1/\mu^\circ = 50$ ,  $\varphi^\downarrow = 0.4$ ,  $\varphi^\circ = 0.005$ ,  $m^\downarrow = 4 \times 10^6$ ,  $m^\circ = 0.01$ . We considered three sets of summary values: (B) ILI annual attack rates (aILI, cumulated seasonal ILI data divided by population size) for the simulated and empirical ILI data, (C) the logarithm of the first order differences of aILI (fdILI), and (not shown) population-level incidence attack rates (aINC). (D) QQ-plots for the odd values of aILI, fdILI and aINC versus the normal distribution for a pseudo data set. (E) ABC\* level sets were reconstructed as a by-product of the MCMC algorithm to check if the link function is bijective. (left) The reconstructed level set for the odd aILI (black) is cut orthogonally by the level set for the odd fdILI (blue). (right) The resulting line (grey) is cut by the level set for the odd aINC. The remaining level sets did not reduce the resulting small ball close to  $\theta_0$  any further. Thus, a very small subset of model parameters close to  $\theta_0$  maps to  $\rho^*$ , which suggests that  $\mathcal{L}$  is bijective around  $\rho^*$ . The videos can be played if the pdf is opened in Acrobat Reader. (F) The marginal posterior densities of  $\theta$ , estimated with standard ABC for 50 pseudo data sets  $x \sim \theta_0$ . (G) The same using ABC\*. The ABC\* calibrated  $c_k^-$ ,  $c_k^+$  were substantially tighter than those used with standard ABC and we had no choice but to improve our MCMC sampler, leading to substantially more accurate parameter estimates.



Monte Carlo (MCMC) standard ABC sampler based on (2b), and with the  $d_k$ 's set to the difference in the simulated and observed sample means of the even aILI, fdILI and aINC. The  $c_k^-$ ,  $c_k^+$  were set such that our sampler produced a manageable acceptance probability of 5%. We found that the  $\theta$  are identifiable based on the ILI time series data and annual attack rate estimates. However, while the estimated 95% credibility intervals contained  $\theta_0$ , the mean squared error of the posterior mean or  $\hat{\theta}_{\text{abc}}^{\text{MAP}}$  to  $\theta_0$  (averaged over 50 pseudo data sets) was large and depended on the  $c_k^-$ ,  $c_k^+$  (top right in Table 1 and Figure 4).

Now, we used an MCMC ABC\* sampler, combining the six calibrated TOST statistics with the composite approach that is equivalent to (2b). The link function under the six test statistics for the odd and even aILI, fdILI and aINC is a priori unknown. To verify whether  $\mathcal{L}$  is bijective around  $\rho^*$ , we used the relation

$$\mathcal{L}^{-1}(\rho^*) = \bigcap_{k=1}^K \mathcal{L}_k^{-1}(\rho_k^*), \quad K = 6, \quad (18)$$

and estimated  $\mathcal{L}_k^{-1}$  numerically around  $\rho_k^*$  with local polynomial regression techniques as a by-product of ABC\* output (Loader, 1999). The numerical estimates of the level sets  $\mathcal{L}_k^{-1}(\rho_k^*)$  are highly complex and their intersection forms a very small ball, indicating that the link function is bijective around  $\rho^*$  (A3 met; Figures 4E-F). This justifies using the aILI, fdILI and aINC for inference. The TOSTs depend on the sample standard deviation of the  $s_k^{1:m_k}(y)$ . We therefore need to recalibrate  $\tau_k^-$ ,  $\tau_k^+$ ,  $m_k$  and  $c_k^-$ ,  $c_k^+$  at every ABC\* iteration (Figure ??). These  $c_k^-$ ,  $c_k^+$  were considerably tighter than those used in the previous standard ABC sampler (SOM ??). The ABC\* posterior density was much tighter than the one obtained with standard ABC, and the mean square error of the posterior mean or  $\hat{\theta}_{\text{abc}}^{\text{MAP}}$  to  $\theta_0$  (averaged over 50 pseudo data sets) was  $\approx 20$ -fold smaller than previously (bottom right in Table 1 and Figure 4). We could not verify A1 directly. However, adding further summary values such as the initial seasonal growth rates or peak timing did not change the  $\pi_{\text{abc}}(\theta|x)$  considerably, and removing any of the six statistics lead to less robust inference or larger mean square error. A4-A5 are not met, so that overall we expect that some approximation error remains even with the ABC\* calibrations. A re-analysis of the empirical data will be reported elsewhere.

#### 4. Discussion

Despite many recent methodological advances, the accuracy of the basic ABC accept/reject sampler with non-zero tolerances ( $c > 0$  or  $c_k^- < c_k^+$ ) has not been understood even when sufficient statistics are available (Grelaud et al., 2009; Dean et al., 2011; Drovandi et al., 2011; Barnes et al., 2012; Fearnhead and Prangle, 2012; Filippi et al., 2013; Marin et al., 2013). Here, we considered the accuracy of  $\pi_{\text{abc}}(\theta|x)$  in terms of its KL divergence to  $\pi(\theta|x)$  and in terms of the closeness of the MAP estimate  $\hat{\theta}_{\text{abc}}^{\text{MAP}}$  to the one of  $\pi(\theta|x)$ . We showed through three innovations how and when modelling distributions of summary values leads to accurate ABC parameter inference in the classical, computationally feasible setting that  $c > 0$  or  $c_k^- < c_k^+$ , without asymptotic arguments.

First, we constructed a simple, yet appropriate auxiliary probability space through modelling the distribution of summary values, data points on a summary level. Our premise

is that such stable and characteristic features can be extracted from high-dimensional data (Wood, 2010). Then, as in maximum-likelihood based indirect inference (Gouriéroux et al., 1993), the rationale is to control the ABC\* approximation on the auxiliary space and to provide regularity conditions under which  $\pi_{\text{abc}}(\theta|x)$  remains close to  $\pi(\theta|x)$  on the original parameter space. In particular, the link function  $\mathcal{L}$  must be bijective and continuously differentiable, and the determinant of the Jacobian  $|\det \partial \mathcal{L}|$  must be controlled by the amount of data available for accurate MAP estimates. Bijectivity determines the number of tests required ( $K = \dim(\theta)$ ), and choosing different sets of  $K$  summary values influences the smoothness of  $|\det \partial \mathcal{L}|$ . Monte Carlo output can be used to verify A3 based on (18) as well as A4 and hence A5. We were less successful in verifying A6.

Second, the likelihood approximation under the binary ABC\* accept/reject step can be interpreted as the power function of a suitable hypothesis test on the auxiliary space. Note that auxiliary data  $y$  are repeatedly simulated for given  $\theta$  in ABC, so classical techniques can be naturally embedded within this Bayesian framework (Rubin, 1984). Test statistics satisfying A2.1-A2.4 can be constructed for a variety of simple probability models (Wellek, 2003) and replace the arbitrary  $d_k$  and  $S_k$  in standard ABC. It would be useful to extend A2 to more complex probability models. Such extensions could use the large sample theory for equivalence tests (Lehmann and Romano, 2005), or non-parametric tests (Munk and Czado, 1998), or once-and-for-all power simulations.

Third, the free ABC\* parameters of these tests are  $\tau_k^-$ ,  $\tau_k^+$ ,  $m_k$ , and they can be calibrated prior to the accept/reject step such that each power function is very close to the likelihood of each of the observed summary values on the auxiliary space. The critical regions  $c_k^-$ ,  $c_k^+$  of the tests are calculated from the  $\tau_k^-$ ,  $\tau_k^+$ ,  $m_k$ ; plus further statistics of the simulated and observed summary values in case of a composite hypothesis test. They correspond to the standard ABC tolerances and ABC\* specifies them exactly. In particular, the  $c_k^-$ ,  $c_k^+$  are not any longer “adjustable” to obtain a well-mixing algorithm at some unspecified loss in accuracy, as is common practice with standard ABC. It is harder to implement an efficient ABC\* Monte Carlo sampler, but well worth the effort as we demonstrated on the flu example. We also showed that combining the univariate, calibrated tests with the intersection approach leads to a composite likelihood approximation. It seems difficult to adjust for the correlations between summary values except in simple cases such as the Mahalanobis approach. This suggests to focus on identifying and modelling uncorrelated sets of summary values.

The set of assumptions A1-A6 set out when ABC\* with non-zero tolerances ( $c > 0$  or  $c_k^- < c_k^+$ ) can be as accurate as Bayesian computations for which the likelihood is known. Given the previous lack in understanding the basic ABC accept/reject sampler with non-zero tolerances, we feel these assumptions - together with the full specification of the test statistics, the tolerances and the number of simulated summary values - are overall a strength of ABC\*. In our applications, we found that the accuracy of  $\pi_{\text{abc}}(\theta|x)$  suffers most strongly when A3 is not met, strongly when A1 is not met, and considerably less when A2 or A4 are not met. Finally, while the arguments behind ABC\* are at times subtle, our main observation is very simple and intuitive: unless we are comfortable with asymptotic arguments, the ABC accept/reject decision cannot be based on a single value. Understanding and modelling the data - now on a summary level with  $n_k, m_k > 1$  summary values - is key to ABC inference as for all Bayesian computations for which the likelihood is tractable.

## Acknowledgments

We thank Ioanna Manolopoulou and Christian Robert for detailed and thoughtful comments. Epidemiological data was kindly provided by the Netherlands Institute for Health Services Research (NIVEL) and the National Institute for Public Health and the Environment (RIVM), The Netherlands. OR is supported by the Wellcome Trust (fellowship WR092311MF) and AC is supported by the Medical Research Council (fellowship MR/J01432X/1). Computations were performed at the Imperial College High Performance Computing Service, and we thank Simon Burbidge and Matt Harvey for their support.

## References

1. Barnes, C. P., S. Filippi, M. P. Stumpf, and T. Thorne (2012). Considerate approaches to constructing summary statistics for ABC model selection. *Statistics and Computing* 22(6), 1181–1197.
2. Beaumont, M., W. Zhang, and D. Balding (2002). Approximate Bayesian Computation in population genetics. *Genetics* 162, 2025–2035.
3. Berger, R. and J. Hsu (1996). Bioequivalence trials, intersection-union tests and equivalence confidence sets. *Statistical Science* 11(4), 283–319.
4. Cox, N. and K. Subbarao (2000). Global epidemiology of influenza: past and present. *Annual Review of Medicine* 51(1), 407–421.
5. Dean, T. A., A. Singh, S. S. and Jasra, and G. Peters (2011). Parameter estimation for hidden markov models with intractable likelihoods. *arXiv:1103.5399*.
6. Drovandi, C. C., A. N. Pettitt, and M. J. Faddy (2011). Approximate Bayesian computation using indirect inference. *Journal of the Royal Statistical Society: Series C (Applied Statistics)* 60(3), 317–337.
7. Fearnhead, P. and D. Prangle (2012). Constructing summary statistics for approximate Bayesian computation: semi-automatic approximate Bayesian computation. *Journal of the Royal Statistical Society: Series B (Statistical Methodology)* 74(3), 419–474.
8. Filippi, S., C. P. Barnes, J. Cornebise, and M. P. Stumpf (2013). On optimality of kernels for approximate Bayesian computation using sequential Monte Carlo. *Statistical Applications in Genetics and Molecular Biology* 12(1), 87–107.
9. Gouriéroux, C., A. Monfort, and E. Renault (1993). Indirect inference. *Journal of Applied Economics* 8, S85–118.
10. Grelaud, A., C. P. Robert, J.-M. Marin, F. Rodolphe, and J.-F. Taly (2009). ABC likelihood-free methods for model choice in Gibbs random fields. *Bayesian Analysis* 4(2), 317–336.
11. Lehmann, E. and J. Romano (2005). *Testing statistical hypotheses*. Springer.
12. Loader, C. (1999). *Local regression and likelihood*. Springer.

13. Marin, J., N. Pillai, C. Robert, and J. Rousseau (2013). Relevant statistics for Bayesian model choice. *Journal of the Royal Statistical Society: Series B (Statistical Methodology)* to appear.
14. Munk, A. and C. Czado (1998). Nonparametric validation of similar distributions and assessment of goodness of fit. *Journal of the Royal Statistical Society: Series B (Statistical Methodology)* 60(1), 223–241.
15. Pritchard, J., M. Seielstad, A. Perez-Lezaun, and M. Feldman (1999). Population growth of human Y chromosomes: a study of Y chromosome microsatellites. *Molecular Biology and Evolution Biol. Evol.* 16, 1791–1798.
16. Ratmann, O., G. Donker, A. Meijer, C. Fraser, and K. Koelle (2012). Phylodynamic inference and model assessment with Approximate Bayesian Computation: Influenza as a case study. *PLOS Computational Biology* 8(12), e1002835.
17. Rubin, D. B. (1984). Bayesianly justifiable and relevant frequency calculations for the applied statistician. *Annals of Statistics* 12(4), 1151–1172.
18. Schuurmann, D. (1981). On hypothesis testing to determine if the mean of a normal distribution is contained in a known interval. *Biometrics* 37(617), 137.
19. Truscott, J., C. Fraser, S. Cauchemez, A. Meeyai, W. Hinsley, C. Donnelly, A. Ghani, and N. Ferguson (2011). Essential epidemiological mechanisms underpinning the transmission dynamics of seasonal influenza. *Journal of The Royal Society Interface* 9(67), 304–312.
20. Wang, W. (1997). Optimal unbiased tests for equivalence in intrasubject variability. *Journal of the American Statistical Association* 92(439), 1163–1170.
21. Wellek, S. (2003). *Testing statistical hypotheses of equivalence*. CRC Press.
22. Wood, S. (2010). Statistical inference for noisy nonlinear ecological dynamic systems. *Nature* 466(7310), 1102–1104.

# Supplementary Online Material for

## Statistical modelling of summary values leads to accurate Approximate Bayesian Computations

Oliver Ratmann

*Department of Infectious Disease Epidemiology, Imperial College London, Norfolk Place, London W2 1PG, UK. oliver.ratmann@imperial.ac.uk*

Anton Camacho

*London School of Hygiene and Tropical Medicine, Keppel Street, London WC1E 7HT, UK*

Adam Meijer

*RIVM, National Institute for Public Health and the Environment, Centre for Infectious Disease Control, Bilthoven, The Netherlands*

Gé Donker

*NIVEL, Netherlands Institute for Health Services Research, P.O.Box 1568, 3500 BN Utrecht, The Netherlands*

### S1. Univariate equivalence statistics

We abbreviate for convenience  $s_y = s_k^{1:m_k}(y)$  and  $s_x = s_k^{1:n_k}(x)$ , their sample means  $\bar{s}_y, \bar{s}_x$  and standard deviations  $\hat{\sigma}_y, \hat{\sigma}_x$ .

*Location equivalence, normal  $s_x^i, s_y^j$ .* Suppose the  $s_x^i$  and  $s_y^j$ ,  $i = 1, \dots, n$  and  $j = 1, \dots, m$ , are iid normal with means  $\mu_x, \mu(\theta)$  and common, unknown variance  $\sigma^2$ . Consider the maximum likelihood estimate  $\hat{\mu}_x = \bar{s}_x$  of  $\mu_x$ . Following Schuirmann (1981), we reject the one-sample version of the two one-sided test statistics (TOST)

$$T^- = \frac{\bar{s}_y - \hat{\mu}_x - \tau^-}{\hat{\sigma}_y/\sqrt{m}}, \quad T^+ = \frac{\bar{s}_y - \hat{\mu}_x - \tau^+}{\hat{\sigma}_y/\sqrt{m}}$$

when simultaneously  $T^+ < t_{\alpha,df}$  and  $T^- > t_{1-\alpha,df}$  in order to test

$$H_0: \mu(\theta) - \hat{\mu}_x \notin [\tau^-, \tau^+] \text{ versus } H_1: \mu(\theta) - \hat{\mu}_x \in [\tau^-, \tau^+].$$

Here,  $t_{\alpha,df}$  is the lower  $100\alpha$  percentile of a Student t-distribution with  $df = m - 1$  degrees of freedom. The test is size- $\alpha$  (Berger and Hsu, 1996) and centred at  $\rho^* = 0$  when  $\tau^- = -\tau^+$ . In this case, the power of the TOST is

$$P_x(R|\rho) = F_{t_{df,ncp}}\left(\frac{\tau^+}{\hat{\sigma}_y/\sqrt{m}} + t_{\alpha,df}\right) - F_{t_{df,ncp}}\left(-\frac{\tau^+}{\hat{\sigma}_y/\sqrt{m}} - t_{\alpha,df}\right)$$

with  $ncp = \sqrt{m}\rho/\sigma$ , and approximated by replacing  $\sigma$  in  $ncp$  by  $\hat{\sigma}_y$  (Owen, 1965).

*Dispersion equivalence, normal  $s_x^i, s_y^i$ .* See main text.

*Equivalence in autocorrelations, normal  $s_x^i, s_y^j$ .* Suppose the pairs  $(s_x^i, s_x^{i-1}), (s_y^j, s_y^{j-1})$ ,  $i = 2, \dots, n$  and  $j = 2, \dots, m$  are bivariate normal with correlations  $\varrho_x$  and  $\varrho(\theta)$  for fixed  $i$  and  $j$  respectively. Thin to  $(\tilde{s}_x^i, \tilde{s}_x^{i-1}), (\tilde{s}_y^j, \tilde{s}_y^{j-1})$ ,  $i = 1, \dots, \tilde{n}$  and  $j = 1, \dots, \tilde{m}$ , such that these pairs can be considered independent. Compute the sample Pearson correlation coefficients  $r(\tilde{s}_x^i, \tilde{s}_x^{i-1}), r(\tilde{s}_y^j, \tilde{s}_y^{j-1})$  and their Z-transformations  $z_x, z_y$ , using  $z(r) = \text{atanh}(r)$ , which are approximately normal with mean  $\varrho_x, \varrho_y$  and variance  $1/(\tilde{n} - 3)$  (Hotelling, 1953). Let  $\hat{\varrho}_x = z_x$ , which is a slightly biased estimate of  $\varrho_x$  (Hotelling, 1953). We reject the TOSZ

$$T^- = \frac{z_y - \hat{\varrho}_x - \tau^-}{\sqrt{1/(\tilde{m} - 3)}}, \quad T^+ = \frac{z_y - \hat{\varrho}_x - \tau^+}{\sqrt{1/(\tilde{m} - 3)}}$$

for

$$H_0: \quad \varrho(\theta) - \hat{\varrho}_x \notin [\tau^-, \tau^+] \text{ versus } H_1: \quad \varrho(\theta) - \hat{\varrho}_x \in [\tau^-, \tau^+]$$

when simultaneously  $T^+ < u_\alpha$  and  $T^- > u_{1-\alpha}$ , where  $u_\alpha$  is the lower  $100\alpha$  percentile of a standard Normal. Since the one-sided tests are both approximately size- $\alpha$ , the TOSZ is also approximately size- $\alpha$  (Berger and Hsu, 1996). It is centred at  $\rho^* = 0$  when  $\tau^- = -\tau^+$ . Under the normal approximation, the power of the TOSZ is in this case

$$P_x(R|\rho) = F_{\mathcal{N}(0,1)}\left(\frac{\tau^+ - \rho}{\sqrt{1/(\tilde{m} - 3)}} + u_\alpha\right) - F_{\mathcal{N}(0,1)}\left(-\frac{\tau^+ + \rho}{\sqrt{1/(\tilde{m} - 3)}} - u_\alpha\right).$$

## S2. Calibration procedures

For the simple auxiliary probability models considered here, test statistics can be found such that the power function is continuous in  $\rho_k, \tau_k^-, \tau_k^+$  and enjoys monotonicity properties such that calibrations are particularly straightforward. First, for each  $k$ , it is possible to calibrate the tolerances so that the univariate power functions are maximised at the point of equality  $\rho_k^*$ .

**LEMMA 1. (Univariate calibration of  $\tau_k^-$ )** *Suppose A2.1-A2.3 hold true. Consider critical regions  $R_k(\tau^-)$  for tolerance regions  $[\tau^-, \tau_k^+]$  with fixed  $\tau_k^+$  and let  $\rho_k^{\max}(\tau^-) = \arg\max_{\rho_k} P_x(R_k(\tau^-) | \rho_k)$ . Let  $\tau_k^+ > \rho_k^*$  and suppose that  $\varepsilon > 0$  is small. There are  $\tau_l^-, \tau_u^-$  such that  $\rho_k^{\max}(\tau_l^-) < \rho_k^*$  and  $\rho_k^{\max}(\tau_u^-) \geq \rho_k^*$ , and  $\tau_k^-$  such that  $\rho_k^{\max}(\tau_k^-) = \rho_k^*$  can be found with the binary search procedure*

**Calibrate  $\tau_k^-$**

1: **loop**

2: Set  $\tilde{\tau}_k^- \leftarrow (\tau_l^- + \tau_u^-)/2$  and determine  $c_k^-, c_k^+$  that satisfy (??).

3: Compute  $\tilde{\rho}_k^{\max} = \rho_k^{\max}(\tilde{\tau}_k^-)$ .

4: If  $|\tilde{\rho}_k^{\max} - \rho_k^*| < \varepsilon$ , set  $\tau_k^- \leftarrow \tilde{\tau}_k^-$  and stop. Else if  $\tilde{\rho}_k^{\max} > \rho_k^*$ , set  $\tau_u^- \leftarrow \tilde{\tau}_k^-$  and go to line 2.

5: **end loop**

Proof of Lemma 1: Let  $\tau_u^- = \rho_k^*$ . By A2.1, we have  $\rho_k^{\max}(\tau_u^-) \geq \rho_k^*$ . Using A2.3,  $\rho_k^{\max}(\tau^-)$  decreases as  $\tau^-$  decreases, so there is  $\tau_l^-$  such that  $\rho_k^{\max}(\tau_l^-) < \rho_k^*$ . Since  $\tau^- \rightarrow \rho_k^{\max}(\tau^-)$  is continuous, there is exactly one solution  $\tau_k^-$  such that  $\rho_k^{\max} = \rho_k^*$ , and this solution can be found with a binary search algorithm.  $\square$

These calibrations determine  $\tau_k^-$  as a function of  $\tau_k^+$ ,  $m_k$ ; and possibly further statistics  $C$  of the simulated and observed summary values in case of a composite hypothesis test. Second, we calibrate  $\tau_k^+$  for given  $m_k$  (and  $C$  if necessary) such that the univariate power functions are not flat around  $\rho_k^*$ .

**LEMMA 2. (Univariate calibration of  $\tau_k^+$ )** *Suppose A2.1-A2.3 hold true. Consider rejection regions  $R_k(\tau^+)$  for equivalence regions  $[\tau^-, \tau^+]$  such that  $\rho_k^{\max} = \rho_k^*$  and denote the maximal power by  $\gamma(\tau^+) = P_x(R_k(\tau^+) | \rho_k^*)$ . Suppose that  $\varepsilon > 0$  is small. Then, there are  $\tau_l^+, \tau_u^+$  such that  $\gamma(\tau_l^+) < 0.9$  and  $\gamma(\tau_u^+) > 0.9$  and  $\tau_k^+$  can be found by the binary search procedure*

**Calibrate  $\tau_k^+$**

1: **loop**

2: Set  $\tilde{\tau}_k^+ \leftarrow (\tau_l^+ + \tau_u^+)/2$ , calibrate  $\tilde{\tau}_k^-$  as before and denote the corresponding rejection region by  $R_k(\tilde{\tau}_k^+)$ .

3: Compute the maximal power,  $\gamma(\tilde{\tau}_k^+)$ .

4: If  $|\gamma(\tilde{\tau}_k^+) - 0.9| < \varepsilon$ , set  $\tau_k^+ \leftarrow \tilde{\tau}_k^+$  and stop. Else if  $\gamma(\tilde{\tau}_k^+) < 0.9$ , set  $\tau_l^+ \leftarrow \tilde{\tau}_k^+$  and go to line 2. Else if  $\gamma(\tilde{\tau}_k^+) > 0.9$ , set  $\tau_u^+ \leftarrow \tilde{\tau}_k^+$  and go to line 2.

5: **end loop**

Proof of Lemma 2: Let  $\tau_l^+ = \rho_k^*$ . By Lemma 1, the calibrated  $\tau_l^-$  is also  $\rho_k^*$ . Since  $T_k$  is continuous and level- $\alpha$ , we have  $\gamma(\tau_l^+) \leq \alpha$  which is of course smaller than 0.9. We next show that  $\tau_k^+ \rightarrow \gamma(\tau_k^+)$  is monotonically increasing with  $\tau_k^+$ . Consider  $\tau_1^+ < \tau_2^+$  along with two tests  $\phi_1(y) = \mathbb{1}\{c_1^- \leq T(y) \leq c_1^+\}$ ,  $\phi_2(y) = \mathbb{1}\{c_2^- \leq T(y) \leq c_2^+\}$  for equivalence regions  $[\tau_1^-, \tau_1^+]$  and  $[\tau_1^-, \tau_2^+]$ . Let  $\tau_1^-$  be calibrated for  $\tau_1^+$ . Let  $\psi(y) = \phi_2(y) - \phi_1(y)$ . By Lemmas 3.7.1 and 3.4.2(iv) in (Lehmann and Romano, 2005),  $\psi \neq 0$  and  $\mathbb{E}_\rho \psi(y) > 0$  for all  $\rho > \tau_1^-$ . Consider now  $\phi_3(y) = \mathbb{1}\{c_3^- \leq T(y) \leq c_3^+\}$  for  $[\tau_2^-, \tau_2^+]$  such that  $\tau_2^-$  is calibrated for  $\tau_2^+$ . We have  $\tau_2^- < \tau_1^-$  by Lemma 1. Repeating the same argument as above, we obtain  $\mathbb{E}_\rho \phi_3(y) > \mathbb{E}_\rho \phi_2(y)$  for all  $\rho > \tau_2^-$ . This implies in particular  $\gamma(\tau_1^+) < \gamma(\tau_2^+)$ . Thus, there is  $\tau_u^+$  such that  $\gamma(\tau_u^+) > 0.9$ . By A2.1,  $\tau^+ \rightarrow \gamma(\tau^+)$  is continuous. Hence, there is  $\tau_k^+$  such that  $\gamma(\tau_k^+) = 0.9$  and this  $\tau_k^+$  can be found with a binary search procedure.  $\square$

The ABC approximation is now correctly centred but  $\pi_{\text{abc}}(\theta|x)$  may still be broader than  $\pi(\theta|x)$  due to the diluting effect of the tolerances  $\tau_k^- < \tau_k^+$ . In this case, we also calibrate the number  $m_k$  of simulated data points used for each  $T_k$  (given further statistics  $C$  if a composite hypothesis test is used).

**LEMMA 3. (Univariate calibration of  $m_k$ )** *Suppose A2.1-A2.4 hold true. Consider rejection regions  $R_k(m_k)$  for  $m_k$  simulated and  $n$  observed summary values such that  $\rho_k^{\max} = \rho_k^*$  and  $P_x(R_k(\tau_l^+) | \rho_k^*) = 0.9$ . Denote the signed Kullback-Leibler divergence between the probability densities associated with the summary likelihood and the power function by*

$$\kappa(m_k) = \text{sign} \{ \text{KL}(m_k + 1) - \text{KL}(m_k) \} \text{KL}(m_k)$$

where

$$\text{KL}(m_k) = \int \log \left( \frac{\ell(s_k^{1:n_k} | \rho_k) / C_\ell}{P_x(R_k(m_k) | \rho_k) / C_{\text{abc}}} \right) \ell(s_k^{1:n_k} | \rho_k) / C_\ell d\rho_k$$

and  $C_\ell = \int \ell(s_k^{1:n_k} | \rho_k) d\rho_k$  and  $C_{\text{abc}} = \int P_x(R_k(m_k) | \rho_k) d\rho_k$ . There is  $m_u$  such that  $\kappa(m_u) > 0$  and  $m_k$  can be found by the binary search procedure

**Calibrate**  $m_k$

- 1: Set  $m_l \leftarrow n$ .
- 2: If  $\kappa(m_l) > 0$ , set  $m_k \leftarrow m_l$  and stop.
- 3: **for**  $j = 1 \dots J$  **do**
- 4:   Set  $\tilde{m}_k \leftarrow \text{int}((m_l + m_u)/2)$ , calibrate  $\tilde{\tau}_k^-, \tilde{\tau}_k^+$  as before and denote the corresponding rejection region by  $R_k(\tilde{m}_k)$ .
- 5:   Compute the signed Kullback-Leibler divergence,  $\kappa(\tilde{m}_k)$ .
- 6:   If  $m_l = m_u$  or  $j = J$ , set  $m_k \leftarrow \tilde{m}_k$  and stop. Else if  $\kappa(\tilde{m}_k) < 0$ , set  $m_l \leftarrow \tilde{m}_k$  and go to line 4. Else if  $\kappa(\tilde{m}_k) > 0$ , set  $m_u \leftarrow \tilde{m}_k$  and go to line 4.
- 7: **end for**

Proof of Lemma 3: Consider the densities

$$f(\rho_k) = \ell(s_k^{1:n_k} | \rho_k) / \int \ell(s_k^{1:n_k} | \rho_k) d\rho_k$$

$$f_{\text{abc}}(\rho_k; m) = P_x(R_k(m) | \rho_k) / \int P_x(R_k(m) | \rho_k) d\rho_k$$

for calibrated  $\tau_k^-, \tau_k^+$ . If  $\kappa(n_k) > 0$ , then  $m_k \leftarrow n_k$  is found. We now suppose that  $\kappa(n_k) < 0$ . We first show that  $\kappa(m)$  is monotonically increasing with  $m$ . Since  $T_k$  is consistent, we have for fixed  $\tau^-, \tau^+$  that  $P_x(R_k(m+1) | \rho_k)$  is larger than  $P_x(R_k(m) | \rho_k)$  for all  $\rho_k$ . This implies by Lemma 2 that the calibrated  $[\tau_k^-(m+1), \tau_k^+(m+1)]$  is inside the calibrated  $[\tau_k^-(m), \tau_k^+(m)]$ . To compare the power of the calibrated tests  $\phi_m(y) = \mathbb{1}\{c_k^-(m) \leq T_k(y; m) \leq c_k^+(m)\}$  and  $\phi_{m+1}(y)$ , note that  $\psi(y) = \phi_{m+1}(y) - \phi_m(y) \leq 0$  is non-zero, and that  $\mathbb{E}_{\rho_k^*} \psi(y) = 0$ ,  $\mathbb{E}_{\tau_k^-(m+1)} \psi(y) < 0$ ,  $\mathbb{E}_{\tau_k^+(m+1)} \psi(y) < 0$ . Along the lines of Lemma 3.4.2(iv) in (Lehmann and Romano, 2005), it follows that  $\mathbb{E}_{\rho_k} \psi(y) < 0$  for all  $\rho_k \neq \rho_k^*$ . This implies  $\kappa(m) < \kappa(m+1)$ . In particular, there is  $m_u$  such that  $\kappa(m_u) > 0$ . Since  $\kappa(n_k) < 0$ , there is  $m_k$  that minimises  $|\kappa(m)|$  and this  $m_k$  can be found with a binary search algorithm.  $\square$

### S3. Proofs of the two Theorems

Proof of Theorem ???: Since the prior densities  $\pi(\rho_k)$  are assumed flat, we have for all  $k$  that  $\text{KL}(\pi(\rho_k | x) \| \pi_{\text{abc}}(\rho_k | x)) = \varepsilon_k$ . By A4-A5, we have  $P_x(R | \rho) = \prod_{k=1}^K P_x(R_k | \rho_k)$  and similarly for  $\ell(x | \rho)$  so that  $\text{KL}(\pi(\rho | x) \| \pi_{\text{abc}}(\rho | x)) = \sum_{k=1}^K \varepsilon_k$ . Since the Kullback-Leibler divergence is invariant under parameter transformations, the claim follows with A1-A3.  $\square$

Proof of Theorem ???: Following the calibration of all  $\tau_k^-$ , the univariate power functions have a mode at  $\rho_k^*$ . By A4, the mode of the multivariate  $\rho \rightarrow P_x(R | \rho)$  is  $\rho^* = (\rho_1^*, \dots, \rho_K^*)$ . By A5, the MLE of the multivariate  $\rho \rightarrow \ell(x | \rho)$  is also  $\rho^*$ . Since  $\mathcal{L}$  is bijective, the ABC\* MLE is also the same as the exact MLE. Next, we have that  $\pi_\rho$  does not change the



location of the modes of  $P_x(R|\rho)$  and of  $\ell(x|\rho)$ , so the modes of  $\pi_{\text{abc}}(\rho|x) \propto P_x(R|\rho)\pi_\rho(\rho)$  and  $\pi(\rho|x) \propto \ell(x|\rho)\pi_\rho(\rho)$  are again  $\rho^*$ . Since  $|\partial\mathcal{L}(\theta)| - |\partial\mathcal{L}(\theta^*)|$  grows slower than  $P_x(R|\rho)$  decays around  $\rho^*$ , the mode of  $\pi_{\text{abc}}(\theta|x)$  is  $\mathcal{L}^{-1}(\rho^*)$ . We suppose that the power of the test is broader than  $\ell(s_k|\rho_k)$ , so that  $\ell(s_k|\rho_k)$  also controls the change of variables. Therefore, the mode of  $\pi(\theta|x)$  is also  $\mathcal{L}^{-1}(\rho^*)$ .  $\square$

## S4. Further details on the moving average example

### S4.1. Prior density $\pi(\theta)$

We assume a uniform prior on  $\rho = (\rho_1, \rho_2) \sim U([\rho_1^-, \rho_1^+] \times [\rho_2^-, \rho_2^+])$ . To obtain the prior induced on  $\theta = (a, \sigma^2)$  we decompose the joint pdf as follows:

$$f(a, \sigma^2) = f(\sigma^2|a)f(a)$$

where  $f$  is a generic density specified by its arguments.

#### S4.1.1. Calculation of $f(\sigma^2|a)$

We define the following link function,  $\mathcal{L}_{a, \hat{\nu}_{x1}} : \sigma^2 \rightarrow \rho_1 = (1 + a^2)\sigma^2/\hat{\nu}_{x1}$ , which is monotonically increasing on  $\mathbb{R}^+$  and whose inverse is  $\mathcal{L}_{a, \hat{\nu}_{x1}}^{-1} : \rho_1 \rightarrow \sigma^2 = \hat{\nu}_{x1}\rho_1/(1 + a^2)$ . Since  $\mathcal{L}_{a, \hat{\nu}_{x1}}^{-1}$  is linear on  $\rho_1$  we have:

$$f(\sigma^2|a) = \begin{cases} \frac{1+a^2}{\hat{\nu}_{x1}(\rho_1^+ - \rho_1^-)} & \text{if } \sigma^2 \in [\mathcal{L}_{a, \hat{\nu}_{x1}}^{-1}(\rho_1^-), \mathcal{L}_{a, \hat{\nu}_{x1}}^{-1}(\rho_1^+)] \\ 0 & \text{otherwise.} \end{cases} \quad (\text{S1})$$

#### S4.1.2. Calculation of $f(a)$

We first compute the cdf  $F(a)$  and then differentiate it to obtain the pdf  $f(a)$ . We define the following link function,  $\mathcal{L}_{\hat{\nu}_{x2}} : a \rightarrow \rho_2 = \text{atanh}(a/(1 + a^2)) - \text{atanh}(\hat{\nu}_{x2})$  which is monotonically increasing on  $[-0.5, 0.5]$  and whose inverse is

$$\mathcal{L}_{\hat{\nu}_{x2}}^{-1} : \rho_2 \rightarrow a = \begin{cases} 0 & \text{if } \rho_2 = -\text{atanh}(\hat{\nu}_{x2}), \\ \frac{1 - \sqrt{1 - 4 \tanh(\rho_2 + \text{atanh}(\hat{\nu}_{x2}))}}{2 \tanh(\rho_2 + \text{atanh}(\hat{\nu}_{x2}))} & \text{otherwise.} \end{cases}$$

We can now compute:

$$F(a) = \begin{cases} 0 & \text{if } a < \mathcal{L}_{\hat{\nu}_{x2}}^{-1}(\rho_2^-), \\ \frac{\mathcal{L}_{\hat{\nu}_{x2}}(a) - \rho_2^-}{\rho_2^+ - \rho_2^-} & \text{if } a \in [\mathcal{L}_{\hat{\nu}_{x2}}^{-1}(\rho_2^-), \mathcal{L}_{\hat{\nu}_{x2}}^{-1}(\rho_2^+)], \\ 1 & \text{if } a > \mathcal{L}_{\hat{\nu}_{x2}}^{-1}(\rho_2^+), \end{cases}$$

and thus:

$$f(a) = \left. \frac{dF(x)}{dx} \right|_a = \begin{cases} \frac{1-a^2}{(1+a^2+a^4)(\rho_2^+ - \rho_2^-)} & \text{if } a \in [\mathcal{L}_{\hat{\nu}_{x2}}^{-1}(\rho_2^-), \mathcal{L}_{\hat{\nu}_{x2}}^{-1}(\rho_2^+)], \\ 0 & \text{otherwise.} \end{cases} \quad (\text{S2})$$

**S4.1.3. Calculation of  $f(a, \sigma^2)$** 

Combining equations (S1) and (S2) we obtain:

$$f(a, \sigma^2) = \begin{cases} \frac{1-a^4}{(1+a^2+a^4)(\rho_2^+-\rho_2^-)\hat{\nu}_{x1}(\rho_1^+-\rho_1^-)} & \text{if } a \in [\mathcal{L}_{\hat{\nu}_{x2}}^{-1}(\rho_2^-), \mathcal{L}_{\hat{\nu}_{x2}}^{-1}(\rho_2^+)] \\ & \text{and } \sigma^2 \in [\mathcal{L}_{a, \hat{\nu}_{x1}}^{-1}(\rho_1^-), \mathcal{L}_{a, \hat{\nu}_{x1}}^{-1}(\rho_1^+)], \\ 0 & \text{otherwise.} \end{cases} \quad (\text{S3})$$

From a practical point of view it is more natural to parametrize the prior on  $\theta$  by specifying boundaries for  $a$  and  $\sigma^2$  rather than for  $\rho_1$  and  $\rho_2$ . For given boundaries  $[a^-, a^+] \times [\sigma^{-2}, \sigma^{+2}]$  on  $\theta$  we propose to choose the following boundaries for the uniform prior on  $\rho$ :

$$\begin{cases} \rho_1^- = \operatorname{argmin}_{\theta}(\mathcal{L}_{a, \hat{\nu}_{x1}}(\sigma^2)) = \mathcal{L}_{1, \underline{a}, \hat{\nu}_{x1}}(\sigma^{-2}) \text{ with } \underline{a} = \operatorname{argmin}_{a \in [a^-, a^+]}(|a|), \\ \rho_1^+ = \operatorname{argmax}_{\theta}(\mathcal{L}_{a, \hat{\nu}_{x1}}(\sigma^2)) = \mathcal{L}_{1, \bar{a}, \hat{\nu}_{x1}}(\sigma^{+2}) \text{ with } \bar{a} = \operatorname{argmax}_{a \in [a^-, a^+]}(|a|), \\ \rho_2^- = \operatorname{argmin}_{\theta}(\mathcal{L}_{\hat{\nu}_{x2}}(a)) = \mathcal{L}_{\hat{\nu}_{x2}}(a^-), \\ \rho_2^+ = \operatorname{argmax}_{\theta}(\mathcal{L}_{\hat{\nu}_{x2}}(a)) = \mathcal{L}_{\hat{\nu}_{x2}}(a^+), \end{cases} \quad (\text{S4})$$

which ensures that the prior induced on  $\theta$  contains the rectangle  $[a^-, a^+] \times [\sigma^{-2}, \sigma^{+2}]$ . With these bounds the expression of  $f(a, \sigma^2)$  becomes:

$$f(a, \sigma^2) = \begin{cases} \frac{1-a^4}{(1+a^2+a^4) \operatorname{atanh}\left(\frac{a^+-a^-}{1-(a^++a^-)}\right) ((1+\bar{a}^2)\sigma^{+2} - (1+\underline{a}^2)\sigma^{-2})} & \text{if } a \in [a^-, a^+] \\ & \text{and } \sigma^2 \in \left[\frac{1+a^2}{1+a}\sigma^{-2}, \frac{1+\bar{a}^2}{1+\bar{a}}\sigma^{+2}\right], \\ 0, & \text{otherwise.} \end{cases} \quad (\text{S5})$$

An example of prior induced on  $\theta$  is shown in Figure S3.

**S4.2. Markov Chain Monte Carlo algorithm for estimating  $\pi(\theta|x_{1:n})$** 

When inferring the parameters  $\theta = (a, \sigma^2)$  of  $x_{1:n} \sim MA(1)$ , the past white noise  $u_0$  needs also to be inferred. However, since we used simulated data and were interested in the exact posterior of  $\theta$  we simply fixed  $u_0 = 0$  and used the likelihood of  $x_{1:n}$  conditional on  $u_0$  given by Marin and Robert (2007):

$$l^c(a, \sigma^2|x_{1:n}, u_0) \propto \sigma^{-n} \prod_1^n \exp\left(-\frac{\hat{u}_t^2}{2\sigma^2}\right), \quad (\text{S6})$$

where the  $\hat{u}_t (t > 0)$  are given by the recursive formula:

$$\hat{u}_t = x_t - a\hat{u}_{t-1}.$$

We implemented a Metropolis-Hasting MCMC algorithm with a bivariate gaussian kernel proposal truncated to the natural support of  $\theta$ :  $[-0.5, 0.5] \times \mathbb{R}^+$  and with covariance matrix:

$$\Sigma_{\theta} = \begin{pmatrix} 5 \times 10^{-2} & 5 \times 10^{-4} \\ 5 \times 10^{-4} & 5 \times 10^{-2} \end{pmatrix}.$$

leading to an acceptance rate of  $\sim 20\%$ . We ran and combined 6 chains for  $2 \times 10^6$  iterations, starting near the true parameter values.

### S4.3. ABC\* subsetting procedure

We considered the following subsets for given time series data  $x_{1:n}$ . First, autocorrelations in  $x_{1:n}$  were ignored, leading to  $s_1^i = x^i$ ,  $i = 1, \dots, n$  and  $s_2 = (x_1, x_2), (x_2, x_3), \dots, i = 1, \dots, n$  for the variance and correlation test respectively. Second, we thinned  $x_{1:n}$  to  $s_{1a}^i = x^{2i-1}$  and  $s_{1b}^i = x^{2i}$ ,  $i = 1, \dots, n/2$  for two variance tests, and used  $s_{2a} = (x_1, x_2), (x_4, x_5), (x_7, x_8), \dots$  and  $s_{2b} = (x_2, x_3), (x_5, x_6), (x_8, x_9), \dots$  and  $s_{2c} = (x_3, x_4), (x_6, x_7), (x_9, x_{10}), \dots$  for three correlation tests.

### S4.4. Influence of the link function

The rate of change  $|\det \partial \mathcal{L}|$  is non-linear and may compromise the accuracy of point estimates of  $\pi_{\text{abc}}(\theta | x_{1:n})$ . This is particularly so when  $P_x(R|\rho)$  is broad so that  $|\det \partial \mathcal{L}|$  has considerable support to act on. To illustrate, we increased the sample size  $n$  but did not re-calibrate  $\tau_k^+$ , expecting that  $\hat{\theta}_{\text{abc}}^{\text{MAP}}$  is increasingly inaccurate as the power function plateaus at one. We ran ABC\* for different pseudo data sets that increase from  $n = m = 500$  to  $n = m = 10^5$ . The  $\hat{\theta}_{\text{abc}}^{\text{MAP}}$  was indeed increasingly inaccurate when the  $\tau_k^+$  are not re-calibrated for each  $m$  (light gray dots in Figure S4D). We repeated inference, now with the  $\tau_k^+$  re-calibrated so that power peaks at 0.9. There was no systematic difference between  $\hat{\theta}_{\text{abc}}^{\text{MAP}}$  and the exact MAP estimate (A6 met, dark gray dots in Figure S4D). The amount of data available controlled  $|\det \partial \mathcal{L}|$  and the calibrations ensured that the ABC\* MAP estimate was very close to  $\hat{\theta}^{\text{MAP}}$  (A6 met; Figure S4D-E).

## S5. Advanced ABC\* algorithms

### S5.1. Markov Chain Monte Carlo algorithm (MCMC)

The MCMC algorithm follows from (Marjoram et al., 2003). Set initial values  $\theta^0$ , compute  $y^0 \sim \ell(\cdot | \theta^0)$  and  $z_k^0 = T_k(s_k^{1:m_k}(y^0), s_k^{1:n_k}(x))$  for all  $k$ . We suppose that  $c_k^- \leq z_k^0 \leq c_k^+$  for all  $k$ .

**ABC\*-m1** If now at  $\theta$ , propose  $\theta'$  according to a proposal density  $q(\theta \rightarrow \theta')$ .

**ABC\*-m2** Simulate  $y' \sim \ell(\cdot | \theta')$ , extract  $s_k^{1:m_k}(y')$  for all  $k = 1, \dots, K$ .

**ABC\*-m3** Compute  $z'_k = T_k(s_k^{1:m_k}(y'), s_k^{1:n_k}(x))$  for all  $k$ .

**ABC\*-m4** Accept  $(\theta', z')$  with probability

$$mh(\theta, z; \theta', z') = \min \left\{ 1, \frac{q(\theta' \rightarrow \theta)}{q(\theta \rightarrow \theta')} \times \frac{\pi(\theta')}{\pi(\theta)} \times \prod_{k=1}^K \mathbb{1}\{c_k^- \leq z'_k \leq c_k^+\} \right\},$$

and otherwise stay at  $(\theta, x)$ . Return to ABC\*-m1.

Throughout, we used a Gaussian proposal kernel. Annealing procedures were added to the covariance matrix of the Gaussian proposal kernel and the tolerances  $\tau_k^-$ ,  $\tau_k^+$  during burn-in.

For the influenza time series example, we previously used a standard ABC MCMC algorithm with annealing schemes on the covariance matrix of a Gaussian proposal matrix and the tolerances. The covariance matrix was diagonal. For ABC\*, the calibrated  $c_k^-$ ,  $c_k^+$  were considerably smaller than those used previously in the standard ABC routine, and we were forced to improve the MCMC sampler. We estimated a more suitable covariance matrix for the proposal density from a sequence of pilot runs, and also employed an annealing scheme on the covariance matrix as well as the tolerances  $\tau_k^-$ ,  $\tau_k^+$ .

### S5.2. Sequential Importance sampling algorithm

This algorithm follows in analogy to the above from (Toni et al., 2008).

## S6. Supplementary Figures

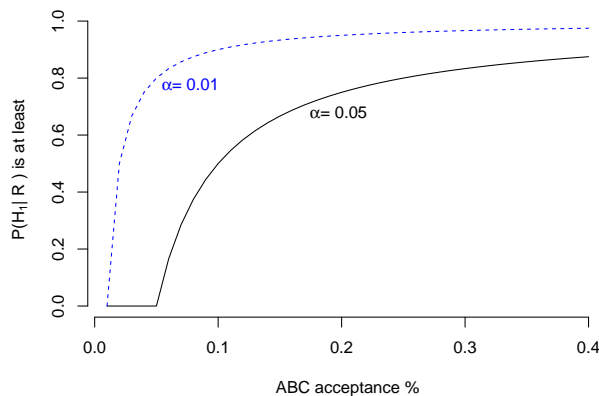


**Fig. S1. Lower bound of ABC true positives.** The true positive ABC\* samples among all accepted ABC\* samples after completion of the algorithm are those  $\theta$  for which  $\rho = \mathcal{L}(\theta)$  is in the equivalence region  $H_1$ . We obtain from Bayes Theorem that the percentage of true positive ABC\* samples is bounded below by  $P_x(H_1|R) = 1 - P_x(H_0|R) \geq 1 - \alpha/P_x(R)$ . The lower bound on the probability of correctly rejecting a level- $\alpha$  equivalence test statistic (i. e.  $1 - P_x(H_0|R)$ ) is plotted as a function of the ABC\* acceptance probability  $P_x(R)$  for  $\alpha = 0.01$  (blue) and  $\alpha = 0.05$  (black). Since the ABC\* acceptance probability rarely exceeds 20%, we fix  $\alpha = 0.01$ . In this case, if the ABC\* acceptance probability is smaller than 2%, then the percentage of true positive ABC\* samples could be as low as 50%

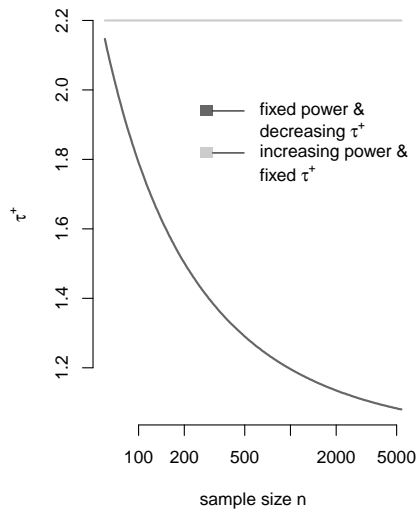


**Fig. S2.** ABC\* inference of  $\sigma^2$  under calibrated tolerances  $\tau^- < \tau^+$ . Calibrated upper tolerance  $\tau^+$  as a function of  $m$  (dark gray). The dark gray  $\hat{\theta}_{\text{abc}}^{\text{MAP}}$  estimates in Figure ??F were obtained from an ABC\* run with these calibrated upper tolerances. The light gray  $\hat{\theta}_{\text{abc}}^{\text{MAP}}$  estimates in Figure ??F were obtained from an ABC run with fixed upper tolerance (shown here also in light gray).

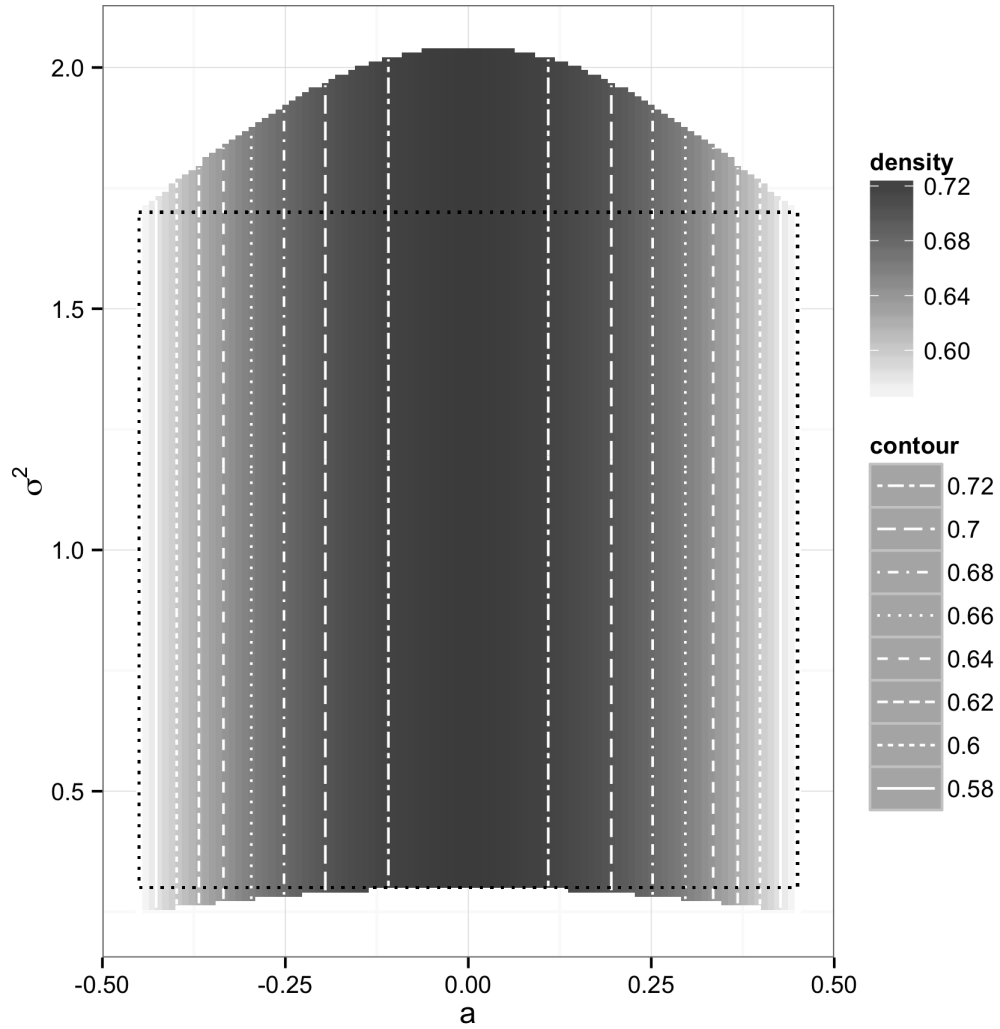


**Fig. S3.** Prior on  $\theta = (a, \sigma^2)$  induced by an uniform prior on  $\rho = (\rho_1, \rho_2)$ , as given by equation (S5). The boundaries of the uniform prior on  $\rho$  are computed using equations (S4) with  $a^- = -0.43$ ,  $a^+ = 0.43$ ,  $\sigma^{-2} = 0.3$  and  $\sigma^{+2} = 1.7$ , which ensure that the prior induced on  $\theta$  contains the rectangle  $[a^-, a^+] \times [\sigma^{-2}, \sigma^{+2}]$  (black dotted line). Here, we have fixed the variance  $\hat{\nu}_{x_1} = (1 + a^2)\sigma^2$  and autocorrelation  $\hat{\nu}_{x_2} = a \tanh(a/(1 + a^2))$  to their theoretical values and obtained the following uniform prior  $(\rho_1, \rho_2) \sim U[(-0.493, 0.294) \times (0.297, 2.024)]$ . Note that the prior induced on  $\theta$  is rather uninformative.

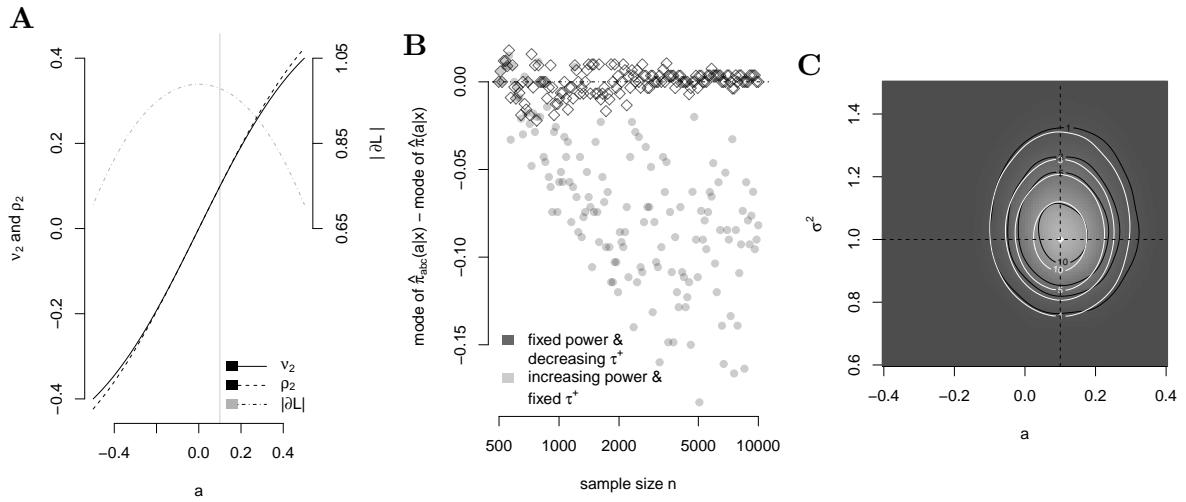


**Fig. S4. Link function and ABC\* inference for the MA(1) model.** (A) The link function (black) and  $|\det \partial\mathcal{L}|$  (gray) as a function of  $a$ .  $|\det \partial\mathcal{L}|$  increases to the left of  $a_0 = 0.1$  (vertical grey line). (B) We increased the sample size  $n$  but did not re-calibrate  $\tau_k^+$ , expecting that  $\hat{\theta}_{\text{abc}}^{\text{MAP}}$  is increasingly inaccurate as the power function plateaus at one. The  $\hat{\theta}_{\text{abc}}^{\text{MAP}}$  was indeed increasingly inaccurate when the  $\tau_k^+$  are not re-calibrated for each  $m$  (light gray dots). We repeated inference, now with the  $\tau_k^+$  re-calibrated so that power peaks at 0.9. There was no systematic difference between  $\hat{\theta}_{\text{abc}}^{\text{MAP}}$  and the exact MAP estimate (A6 met, dark gray dots). (C) Standard ABC posterior density (black contour) as described in the main text, with tolerances set so that ABC-r acceptance probability was 0.5%. Monte Carlo error becomes noticeable and otherwise ABC approximation is comparable to that of ABC\*.

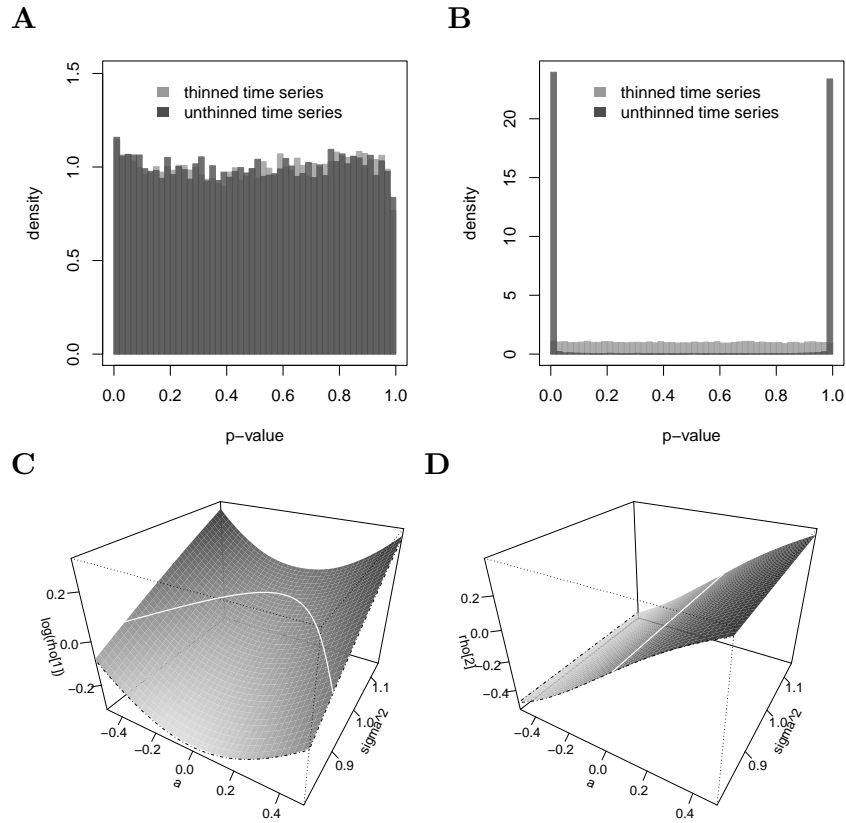


**Fig. S5.** ABC self-assessment for ABC inference on the MA(1) model. We verified during ABC runtime that the test assumptions on the summary values are met. (A) To assess normality, we used the Shapiro-Francia test (Royston, 1993) to compute a p-value at every ABC iteration for each set of summary values. After runtime, the distribution of p-values was tested for departures from  $\mathcal{U}(0, 1)$ . Histograms of p-values are shown for two cases: summary values set to the thinned time series (light gray) and to the time series without thinning (dark gray). (B) To assess if summary values are uncorrelated, we tested for non-zero partial autocorrelations (Box et al., 2011). Histograms are shown for the same two cases. Summary values can be considered uncorrelated only after thinning. Further, we evaluated if the link function can be numerically reconstructed from ABC output with local polynomial regressions. (C) The first dimension of the reconstructed link function  $\hat{\mathcal{L}}_1$  (gray) and true link function  $\mathcal{L}_1$  (black, dashed-dotted, on the sides), with added level set  $\mathcal{L}_1^{-1}(\rho_1^*)$  (white). (D) The second dimension of the reconstructed link function  $\hat{\mathcal{L}}_2$  (gray) and true link function  $\mathcal{L}_2$  (black, dashed-dotted, on the sides), with added level set  $\mathcal{L}_2^{-1}(\rho_2^*)$  (white).



**Table S1.** SEIRS model parameters, priors, and standard ABC and ABC\* posterior densities

description		prior density	mean±std. dev., 95% conf. interval of	
			standard ABC posterior density	ABC* posterior density
			$\theta_0 = (R_0, 1/\gamma, \omega) = (3.5, 10, 0.08)$	
$R_0$	Basic reproductive number	$\mathcal{U}(1, 8)$	3.74±0.39, [3.01, 4.37]	3.51±0.02, [3.47, 3.54]
$1/\phi$	Avg incubation period [day]	0.9 §		
$1/\nu$	Avg infectiousness period [day]	1.8 §		
$1/\gamma$	Avg duration of immunity [year]	$\mathcal{U}(2, 30)$	11.1±1.58, [8.15, 13.76]	9.93±0.07, [9.79, 10.07]
$\omega$	Reporting rate	$\mathcal{U}(0, 1)$	0.092±0.02, [0.058, 0.133]	0.0799±0.0004, [0.0791, 0.0808]
$N^\downarrow$	Size of sink population	$\approx 15 \times 10^6$ varies in time <sup>†</sup>		
$N^\circ$	Size of source population	$\mathcal{U}(1, 10) \times 10^8$	*	*
$\mu^\downarrow$	Birth/death rate of sink population	fixed <sup>†</sup>		
$\mu^\circ$	Birth/death rate of source population, [1/year]	1/50 ¶		
$\varphi^\downarrow$	Seasonal forcing of $\beta_t^\downarrow$	$\mathcal{U}(0.07, 0.6)$	*	*
$\varphi^\circ$	Seasonal forcing of $\beta_t^\circ$	$\mathcal{U}(0, 0.03)$	*	*
$m^\downarrow$	Number of travelers visiting the sink population <sup>†</sup>	$\mathcal{U}(3, 15) \times 10^6$ †	*	*
$m^\circ$	Fraction of $\hat{I}^\circ$ re-seeding the source population	$\mathcal{U}(0, 0.1)$	*	*

$M^\circ$  in the analogue of (??) for the source population is defined by  $M^\circ = m^\circ \hat{I}^\circ$  where  $\hat{I}^\circ$  is the number of infected individuals at disease equilibrium in the source. <sup>†</sup>Fixed to demographic data <http://statline.cbs.nl>. Number of travellers encompass annual records. <sup>§</sup>Fixed to match influenza A (H3N2)'s estimated generation time <sup>¶</sup>Assuming an average lifespan of 60 years, adjusted by net fertility rate in SE Asia \*For the simulated data set, these parameters were fixed to the values reported in Figure ??.

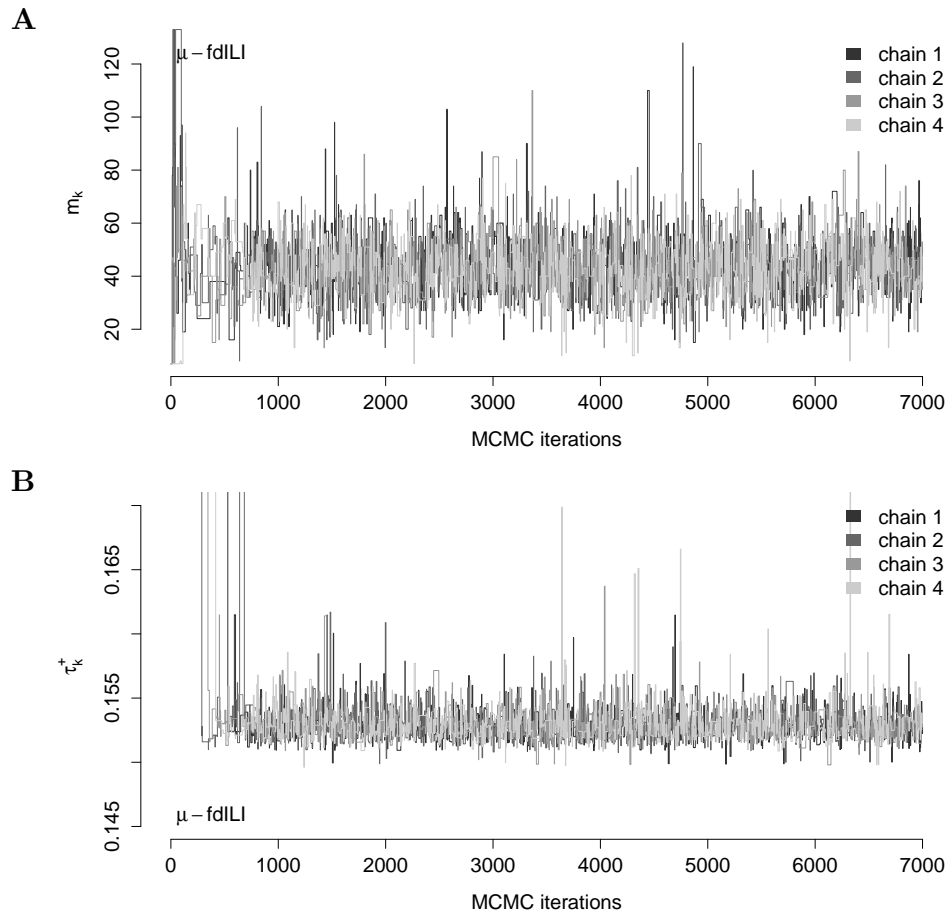


**Fig. S6.** ABC inference on the influenza A (H3N2) data on simulated data - calibrations. ABC\* inference based on the summary values in Figure ???. TOST test statistics were used based on the distribution of the summary values, and MCMC chains were run for 10,000 iterations. The free ABC parameters were re-calibrated at every iteration because the TOST also depends on the standard deviation of the summary values. (A) Calibrated  $m_k$  and (B) calibrated  $\tau_k^+$  for four MCMC chains that were run in parallel from overdistributed starting values.

## References

1. Berger, R. and J. Hsu (1996). Bioequivalence trials, intersection-union tests and equivalence confidence sets. *Statistical Science* 11(4), 283–319.
2. Box, G., G. Jenkins, and G. Reinsel (2011). *Time series analysis: forecasting and control*. Wiley.
3. Hotelling, H. (1953). New light on the correlation coefficient and its transforms. *Journal of the Royal Statistical Society. Series B (Methodological)* 15(2), 193–232.
4. Lehmann, E. and J. Romano (2005). *Testing statistical hypotheses*. Springer.
5. Marin, J.-M. and C. P. Robert (2007). *Bayesian core: a practical approach to computational Bayesian statistics*. Springer.
6. Marjoram, P., J. Molitor, V. Plagnol, and S. Tavaré (2003). Markov Chain Monte Carlo without likelihoods. *Proceedings of the National Academy of Sciences USA* 100(26), 15324–15328.
7. Owen, D. (1965). A special case of a bivariate non-central t-distribution. *Biometrika* 52(3/4), 437–446.
8. Royston, P. (1993). A pocket-calculator algorithm for the Shapiro-Francia test for non-normality: An application to medicine. *Statistics in Medicine* 12(2), 181–184.
9. Schuurmann, D. (1981). On hypothesis testing to determine if the mean of a normal distribution is contained in a known interval. *Biometrics* 37(617), 137.
10. Toni, T., D. Welch, N. Strelkowa, A. Ipsen, and M. P. H. Stumpf (2008). Approximate Bayesian computation scheme for parameter inference and model selection in dynamical systems. *Journal of The Royal Society Interface* 6(31), 187–202.